TALLINNA
TEHNIKAÜLIKOOL

Faculty of Mechanical Engineering
Chair of Technical Mechanics

EMD70LT

Sander Nelis

A SIMPLIFIED MODEL FOR ICE FORCES IN SHIP-ICE COLLISION

Thesis submitted in partial fulfilment
of the requirements for the degree of
Master of Science in Technology

Tallinn
2015

TALLINNA
TEHNIKAÜLIKOOL

Mehaanikateaduskond
Tehnilise mehaanika õppetool

EMD70LT

Sander Nelis

LIHTSUSTATUD MUDEL JÄÄKOORMUSE HINDAMISEKS LAEVA JA JÄÄ KOKKUPÕRKEL

Autor taotleb
tehnikateaduse magistri
akadeemilist kraadi

Tallinn
2015

AUTORIDEKLARATSIOON

Deklareerin, et käesolev lõputöö on minu iseseisva töö tulemus.
Esitatud materjalide põhjal ei ole varem akadeemilist kraadi taotletud.
Töös kasutatud kõik teiste autorite materjalid on varustatud vastavate viidetega.

Töö valmis Kristjan Tabri juhendamisel

“.....”.....2015 a.

Töö autor

..... allkiri

Töö vastab magistritööle esitatavatele nõuetele.

“.....”.....2015 a.

Juhendaja

..... allkiri

Lubatud kaitsmisele.

..... eriala/õppekava kaitsmiskomisjoni esimees

“.....”.....2015 a.

..... allkiri

TTÜ mehaanika instituut
Tehnilise mehaanika õppetool

MAGISTRITÖÖ ÜLESANNE

2014 aasta kevadsemester

Üliõpilane: Sander Nelis, 122180MATMM
Õppekava: MATM02/11 – Tootearendus ja tootmistehnika
Eriala: Laevaehitus
Juhendaja: Kristjan Tabri, D.Sc. (Tallinna Tehnikaülikool)
Konsultandid: Professor Pentti Kujala (Aalto Ülikool)
Jakub Montewka, Ph.D. (Aalto Ülikool)

MAGISTRITÖÖ TEEMA:
Lihtsustatud mudel jääkoormuse hindamiseks laeva ja jää kokkupõrkel
A simplified model for ice forces in ship-ice collision

Lõputöös lahendatavad ülesanded ja nende täitmise ajakava:

Nr	**Ülesande kirjeldus**	**Täitmise tähtaeg**
1	**Magistritöö kava esitamine**	**10.03.14**
2.	**Jääkoormuse mudeli välja arendamine**	**11.05.2014**
3.	**Lihtsustatud kokkupõrke mudeli arendamine**	**08.06.2014**
4.	**Tulemuste esitamine**	**27.07.2014**
5.	**Lõputöö lõplik versioon**	**15.09.2014**

Lahendatavad insenertehnilised ja majanduslikud probleemid:
Magistritöö eesmärk on välja arendada lihtsustatud mudel hindamaks kokkupõrke energiat kahe laeva kokkupõrke puhul võttes arvesse jää olusid, milles meretranspordi süsteem opereerib teatud osa aastast Balti meres. Selleks on vaja tuletada mudel, mis võtaks arvesse jääkoormust laeva ristisuunas kokkupõrkel jääga.

Töö keel: inglise keel
Kaitsmistaotlus esitada hiljemalt 17.12.2014 **Töö esitamise tähtaeg:** 19.01.2015
Üliõpilane Sander Nelis /allkiri/ …….. kuupäev……
Juhendaja Kristjan Tabri /allkiri/ ……. kuupäev……
Konfidentsiaalsusnõuded ja muud ettevõttepoolsed tingimused formuleeritakse pöördel

ACKNOWLEDGEMENTS

This thesis was carried out with the collaboration of Aalto University School of Engineering and Tallinn University of Technology, as a part of WINOIL (Winter Navigation Risks and Oil Contingency Plan) project and project B18: Tool for direct damage calculations for ship collision and grounding accidents, respectively.

I would like to thank Tallinn University of Technology for giving such an opportunity and enabling to obtain a degree at the Aalto University.

I would like to express my sincere gratitude to my supervisor, Professor Pentti Kujala, for his valuable guidance and advices. I am also grateful to my instructor, Ph.D. Jakub Montewka for his guidance and comments in the beginning phase of the thesis.

I sincerely thank my instructor D.Sc. Kristjan Tabri, from Tallinn University of Technology, for his support and valuable advices throughout the thesis writing.

Finally, I am extremely grateful to my family and friends for their endless support, and obviously I would like to thank my dear Marit for her support and encouragement during my degree studies.

Espoo, September 2014

Sander Nelis

TABLE OF CONTENTS

LIST OF SYMBOLS

a	coefficient in the ice force calculations
C	unknown parameter
D	width of the structure
dm	added mass of struck ship in the sway direction
E	Elastic modulus of the ice
E_0	total kinetic energy before collision
E_{Def}	deformation energy
E_{ice}	energy from ice
$E_{K,A}$	striking ship kinetic energy after collision
$E_{K,B}$	struck ship kinetic energy after collision
F_{ice}	ice force that applies to the ship side
g	acceleration due to the gravity,
H	total horizontal ice force
h_i	ice thickness
H_B	breaking force which presents failure
H_R	ice ride-up/ride-down force
M_A	mass of striking ship
M_B	mass of struck ship
M_{ice}	mass of ice

L_{mid}	midship length
l_c	contact length
P_h	horizontal force
P_v	vertical force
q	line load
$q_{Croasdale}$	Croasdale's line load
s	value of the frame spacing
t_{com}	time the ships reach to the common velocity
z	depth of the slope
z^0	global vertical axis
t	time
V_A	initial velocity of the striking ship
V_{com}	final common velocity
x_A	striking ship displacement
x_B	struck ship displacement
α	slope angle of ship's hull
δ	penetration depth
λ	geometric scale factor
ξ	a function of slope angle and the friction coefficient
μ	friction coefficient between ice and structure
ρ_i	density of ice
ρ_w	density of water
σ_f	flexural strength of ice
ϕ	collision angle

ΔKE	total kinetic energy absorbed in the collision

ABBREVIATIONS

FMI	Finnish Meteorological Institute
ISO	International Organization for Standardization
LNG	Liquefied Natural Gas
LPG	Liquefied Petroleum Gas
NBS	Northern Baltic Sea
SAFEWIN	an EU project of Safety of Winter Navigation in Dynamic Ice
SMHI	Swedish Meteorological and Hydrological Institute
WINOIL	Winter Navigation Risks and Oil Contingency Plan

LIST OF FIGURES

LIST OF TABLES

1 INTRODUCTION

1.1 Background

The maritime transportation system in the Northern Baltic Sea (NBS) is complex and operates under varying environmental conditions. The most challenging conditions relate to the presence of ice-cover, which for the NBS i.e. Gulf of Finland or Bay of Bothnia, can remain up to several months. It is also evident, that the number of accidents in these two areas is the highest during winter season which can involve accidents like groundings, collisions and damages due to the ice. In these regions several different ice conditions exist which varies greatly during the winter time. Therefore, ships has to be capable to navigate either by their own or by the help of the icebreaker in the level ice, compressive ice, through the ice ridges and in the ice channels.

Currently, the accidents with ships are mainly studied in the open water, and there exists several models for estimating the consequences of accidents in these conditions. However there is no such solution for the ice-covered waters, although the risk for accidents is in principle the same or even higher. Furthermore, there are made model test for ship-ship collisions in open water, but as far as known for the author of this thesis, there is no available knowledge of any model tests related to the ship-ship collisions in ice. The reason for that is generally the complexity of the ice behaviour and high cost of making any model testing or full scale experiments.

The existence of such a solution would be necessary, as it helps to understand how much the presence of ice affects the ships collision damages and how the collision energy is changed due to that. Based on the knowledge obtained from the collision model in ice, ship structures can be designed and optimized in way that they absorb as much energy as possible to prevent water flooding or oil leakage. It is known, oil spills are difficult problems in ice conditions. Effective oil-combating methods in the ice do not exist, and it is difficult to keep track of where the oil is going. The oil may penetrate into the ice sheet and drift with the ice or drift on the surface of openings and beneath sea ice (Leppäranta & Myrberg, 2009). Therefore, as in the NBS operates a large amount of oil tankers, the pollution risk due to their collision is relatively high. Thus,

having such a model, which includes ice in collision calculations, is a good help in the future studies to estimate the deformation energy due to the impact.

1.2 Aim of the thesis

This thesis aims at the development of a model estimating the collision energy of two ships colliding, taking into account the specific winter regime under which the analysed maritime transportation system is operating. Such model will feed a broader concept of risk assessment, as it ultimately allows determining the consequences of a collision between ships in the presence of ice.

The thesis will focus on studying and developing ice load and collision energy formulas for a collision scenario where ship collides with another at a 90 degrees angle in ice. Due to restricted ability to move sideways after collision, the ship structure will take more energy than in the case where ship can freely move. Sketch of the collision is presented in Figure 1.1.

The developed model will take into account only a constant total horizontal ice force, which based on Croasdale's 2-D approach consists of the bending force and the ride-down force. Although, in the case of vertical hull side, the ice crushing and bending is rather mixed process during sideways movement. Additionally, friction between the ice and the structure is considered in the ride-down force formula. However ice pile accumulating in front of hull side during the collision is not considered.

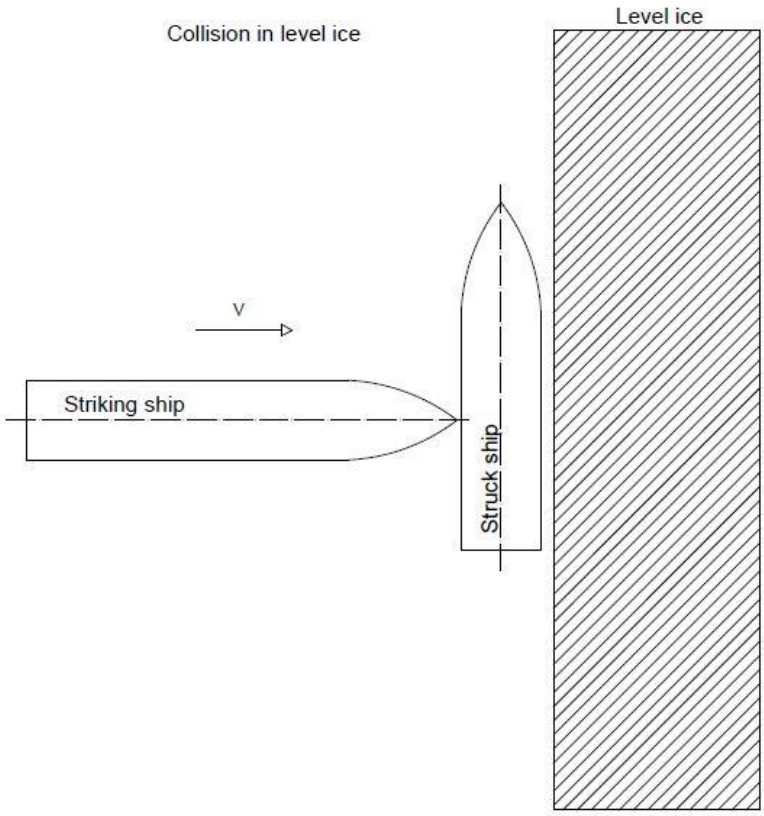

Figure 1.1 Collision sketch at a 90 degree angle.

According to the scenario, it will be studied what kind of ice forces will be acting on ship structures, which in turn causes the interest to investigate the increase of the deformation energy. In addition, attention will be paid on the evaluation of the ice characteristics and ice conditions that are going to be considered.

Finally, the developed ice force calculation model will be compared with available experimental data. The collision results will also be compared with open water outcomes. It is obviously expected that the deformation energy should increase due to the influence of ice.

1.3 State of art

In the last decades the ship collision and grounding accidents has been studied by several researchers, who has been developed collision models either based on conservation of momentum or time-domain model. Minorsky (1959) was first who separated the collision

problem into two parts, as an internal and an external part. His approach includes model where the striking ship moves towards stationary struck ship in perpendicular direction and the momentum conservation is based on the ship masses and velocities before and after the contact. Zhang (1999) managed 40 years later to revise Minorsky method and developed simplified formulas for the relationship between the absorbed energy and the destroyed material volume, as it takes into account structural arrangement, materials properties, and damage patterns. Moreover, Zhang's model allows to simulate also eccentric and oblique angle collisions. However as mentioned earlier, in addition to conservation of momentum methods, there is also available time-domain models, see for example Petersen (1982) and Tabri (2010). These models provide ship motions for each time step considering inertial forces, hydrodynamic forces and hydrostatic force. Time-domain simulation models are more precise compared to the conservation of momentum model as they also include the structural resistance and precise penetration path. Momentum conservation models assume predefined and typically linear penetration path.

Besides ship-ship collisions, the accidents with icebergs are already known from the far past. Therefore, different analytical and numerical studies has been conducted to study the iceberg impact loads that ships experiences because of the collision (Liu, 2011). In the Liu's dissertation the impact was divided into external and internal mechanics. A new formulation of three-dimensional impact mechanics of iceberg and ship collision was developed, which was successfully applied to calculate the energy dissipation in the collision. In addition, a numerical model of iceberg and the new ice material model was developed, where the latter was based on plasticity theory and was strain-rate independent.

Similarly to the ship-iceberg collision, different authors has been studied and developed numerical models for ship-ice interaction, which has helped to gain a knowledge about the process and gives opportunity to study cases that would be difficult or even impossible to investigate analytically. Lubbad and Løset (2011) developed a numerical model to simulate the process of ship-ice interaction in real-time, where only the level-and broken ice features were studied. The ice breaking module calculates the response of the breakable ice floes and estimates their actions on the ship's hull. The model was validated against full-scale data, as real-time simulation results were compared with Norwegian coast guard icebreaker *KV Svalbard*

experimental data (Valkonen, et al., 2008). For comparison, the same vessel was also constructed in the simulator. As a result, the data from the simulation was comparable with the full scale data. Although, these tests were made in relatively low speeds, and in higher speeds the global resistance may change.

It is known that the ice loads in reality varies because the ice conditions are not uniform throughout the area where vessel operates. Therefore, a numerical method was proposed to simulate a ship moving forward, either in uniform or variable ice conditions, where the thickness and ice properties were assumed to be constant or randomly generated by using the Monte-Carlo method (Su, 2011). In the simulation programme, a coupling between the continuous ice loads and the ship's motion were considered and the three-degree-freedom rigid body equations of surge, sway and yaw were solved using numerical integration. In that case, the icebreaking tanker MT Uikku was used in the simulation program to validate numerical results. Furthermore, statistical data characterizing Baltic Sea ice (Kujala, 1994) were applied to randomize the ice conditions. Both, the calculated amplitude values of the ice loads on two local frames, and the distributions of the recorded peak loads were comparable to field measurements (Kotisalo & Kujala, 1999) and (Hänninen, 2003) to the measured statistical distributions, respectively. The model was further developed, as the both global and local ice loads were estimated on ships to get overall performance of ship in the ice.

Previous numerical models, proposed by Lubbad and Løset (2011) and Su (2011), both used non-commercial codes that were developed based on the mechanics of full scale ice which was not valid for model ice. Therefore, Tomac (2013) developed simulation applying model ice parameters (von Bock und Polach & Ehlers, 2013) based on nonlinear finite element method to compare ship resistance obtained from simulations with experimental results in level ice and in a compressive ice channel (Suominen & Montewka, 2012). In the simulation, some parts of the total ice resistance, as resistance from submersion and broken ice pieces, were neglected. However, these were estimated and added later to the total resistance, including also open water resistance. Although the results were generally in a good agreement, the research in this field is still ongoing.

Due to the presence of the ice in the Northern Baltic Sea during the winter time, it is evident that ships might collide with each other also in an ice conditions. Unfortunately, there is lack of

knowledge about these kind of collisions in conditions where the ice exist, and currently the methods how to evaluate ice loads to the ship during the collision are hard to be found. Nevertheless, there are developed several ice resistance models that helps to estimate the loads that comes from ice.

It is known that average ice force in the time domain is mainly defined as the ice resistance. To calculate this force for level ice Lindqvist (1989) developed simplified formulas, where the total ice resistance during the ice-hull interaction process is divided into three components: ice crushing component, ice breaking component and ice floe submersion component. However, it is impossible to apply Lindqvist's model, for example, to the ship collision with another at a 90 degrees angle in ice, as the ship is moving in sideways after collision with low speed, and the ice breaking process is different from the one adopted by Lindqvist.

Considering previously mentioned collision scenario, the ice resistance for similar situation was studied by Zhou (2012). Zhou developed a numerical model to simulate the dynamic ice loads acting on an icebreaking tanker in level ice, considering the action of ice in the vicinity of the waterline caused by breaking of intact ice and the effect of submersion of broken ice floes. In addition, he compared numerical simulations with the model tests in an ice tank (Zhou, et al., 2012), where the ice loads were measured during the different ice drift speeds, ice properties and ice drift angles, For the simulations and model tests three different constant heading angles (0, 45 and 90 degrees) were chosen to compare the results.

2 BALTIC SEA ICE CONDITIONS

2.1 Description of ice conditions

Today the winter navigation in the Baltic Sea is very active, as for example, in Finland more than 80% of the international trade is transported via the sea. Therefore, ships need icebreaker assistance for 3-6 months each winter, although in the mildest winters, this need is restricted to the Gulf of Finland, Gulf of Bothnia, and the Gulf of Riga (Vihma & Haapala, 2009). Further, the winter navigation is strongly increasing and during the last decade the marine traffic in the Baltic has increased by 34% and the trend is expected to continue (Seinä, 2008). The main shipping routes in the Baltic Sea can be seen in Figure 2.1.

Figure 2.1 Main shipping routes in the Baltic Sea (Seinä, 2008).

Studies related to sea ice have been performed for several decades in the Baltic Sea, mainly motivated by the development of winter shipping. Finland and Estonia are the only nations in

the world where all harbours can freeze during the winter, which partly explains the interest in sea ice studies. At its annual maximum extent, the ice covers on average between 190 000 and 217 000 km^2, but there is a large inter-annual variability in the date the freezing begins, thickness, extent, and break-up date (Granskog, et al., 2006). Ice cover in the Baltic Sea is shown in Figure 2.2 and it is well seen how different the ice cover can be during different winters.

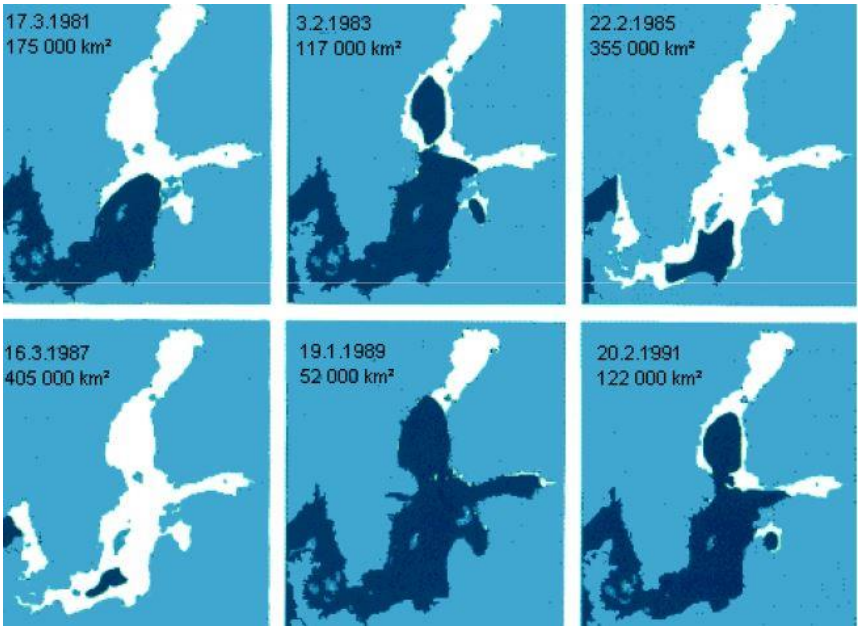

Figure 2.2 Ice extent during different years (Kujala & Riska, 2010).

Ice formation begins at the northernmost Bothnian Bay and the easternmost Gulf of Finland in October-November. During the 20th century, for Kemi the earliest, average and latest freezing dates were October 6, November 10 and December 23, the range covering as much as 2.5 months (Leppäranta & Myrberg, 2009). However, the Bay of Bothnia freezes over on average in mid-January and in normal winters the Sea of Bothnia, the Gulf of Finland and the Gulf of Riga freeze over one month later. Although in mild winters, only the bay of Bothnia and the eastern part of the Gulf of Finland freeze over.

In contrast to freezing, melting begins in the south in early March at the same time as new ice is forming in the north. Melting progress in the central basins is due to the absorption of solar radiation in leads and due to the decrease in ice compactness, and somewhat later melting starts form the shoreline due to the shallow sea depth and the proximity of warm land. In early May,

the ice prevails only in the Bothnian Bay and has completely melted by early June (Granskog, et al., 2006). For instance, in the 20th century, the mean date of ice break-up was May 21 in Kemi, with extremes being April 16 and June 27 (Leppäranta & Myrberg, 2009).

Typically the ice in the Baltic Sea exist as fast ice and drift ice. Fast ice is located in coastal and archipelago areas, where the depth is less than 15 metres. It develops during early ice season and remains stationary to the melting period. The drift ice has a dynamic nature being forced by winds and currents. Drift ice can be either level, rafted or ridged, and its concentration could be 1-100%. Drift ice is occasionally called pack ice if the concentration is more than 80%. Unlike fast ice, drift ice movements are large: in stormy conditions thin drift ice field can move 20-30 km in a single day. The motion results in uneven and broken ice field with distinct floes up to several kilometres in diameter, leads, and cracks, slush and brash ice barriers, rafted ice and ridged ice (The Baltic Sea portal, 2014). The typical ice conditions in the Baltic Sea is presented in Figure 2.3.

However, the ridges and brash ice barriers are the most significant obstructions to navigation in the Baltic Sea. Powerful, ice-strengthened vessels can break through ice up to almost one meter thick, but they are not capable of navigate through ridges without icebreaker assistance. One of the most hazardous situation in the Baltic Sea is the compressive ice fields which is caused by wind, current or tide that puts the ice field into the movement. Therefore, when it hits a barrier, for example a stopped or stuck ship in ice, the stresses will be significant, which in turn might lead to the major damages to the ship structure.

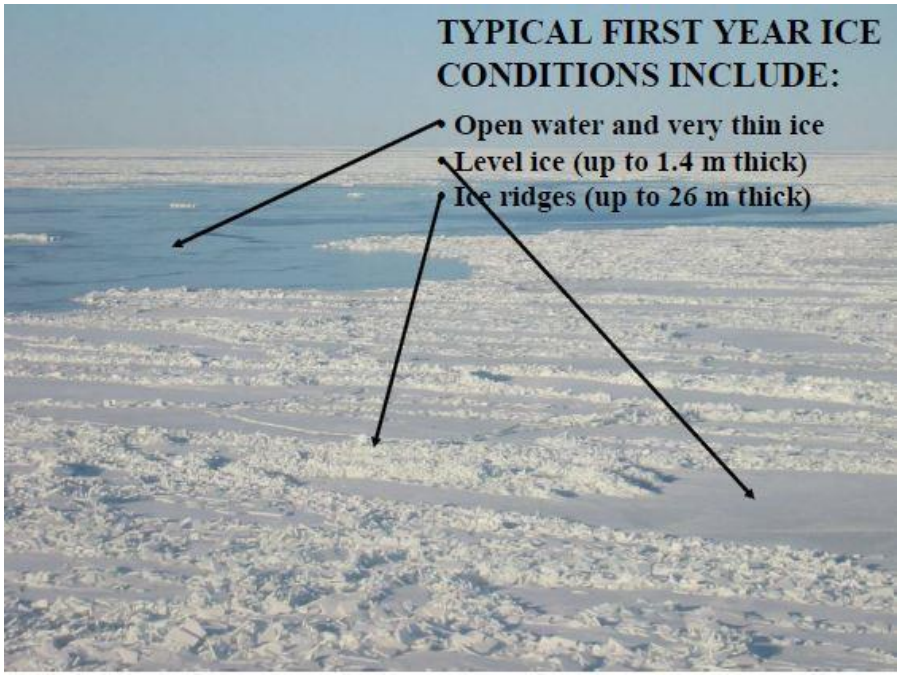

Figure 2.3 Baltic Sea ice conditions (Kujala & Riska, 2010).

2.2 Ice thickness and properties

It is known that in the Baltic Sea only first year ice exist and thickness of the ice cover varies a lot. Well-known is the fact: the thicker the ice is the bigger the ice loads are. Therefore, the thickness of sea ice has a great importance to studies related to ice. The ice cover variation is caused by thermal and mechanical factors. Under the thermal factors are meant the changes in air temperature and snow cover above the ice surface, and the mechanical factors are discrete components caused by rafting, ridging, and opening of leads and polynyas (Kujala, et al., 2007).

The long term variation of level pack ice thickness can be obtained from daily routine ice charts, in which the approximate upper and lower limits of the level ice thickness are given in various parts of the Baltic Sea. Nowadays, it is relatively easy to get information about ice conditions as Finnish Meteorological Institute (FMI) and Swedish Meteorological and Hydrological Institute (SMHI) provides daily updated ice charts for the whole Baltic Sea areas. In Figure 2.4 can be seen the ice chart provided by the SMHI, which gives a good overview about the ice thickness and type in the Bay of Bothnia, Gulf of Finland, and in the Gulf of Riga. As the ice charts are quite informative, these are also widely used by ship crews, who plan their routes based on the charts in order to navigate in milder ice conditions.

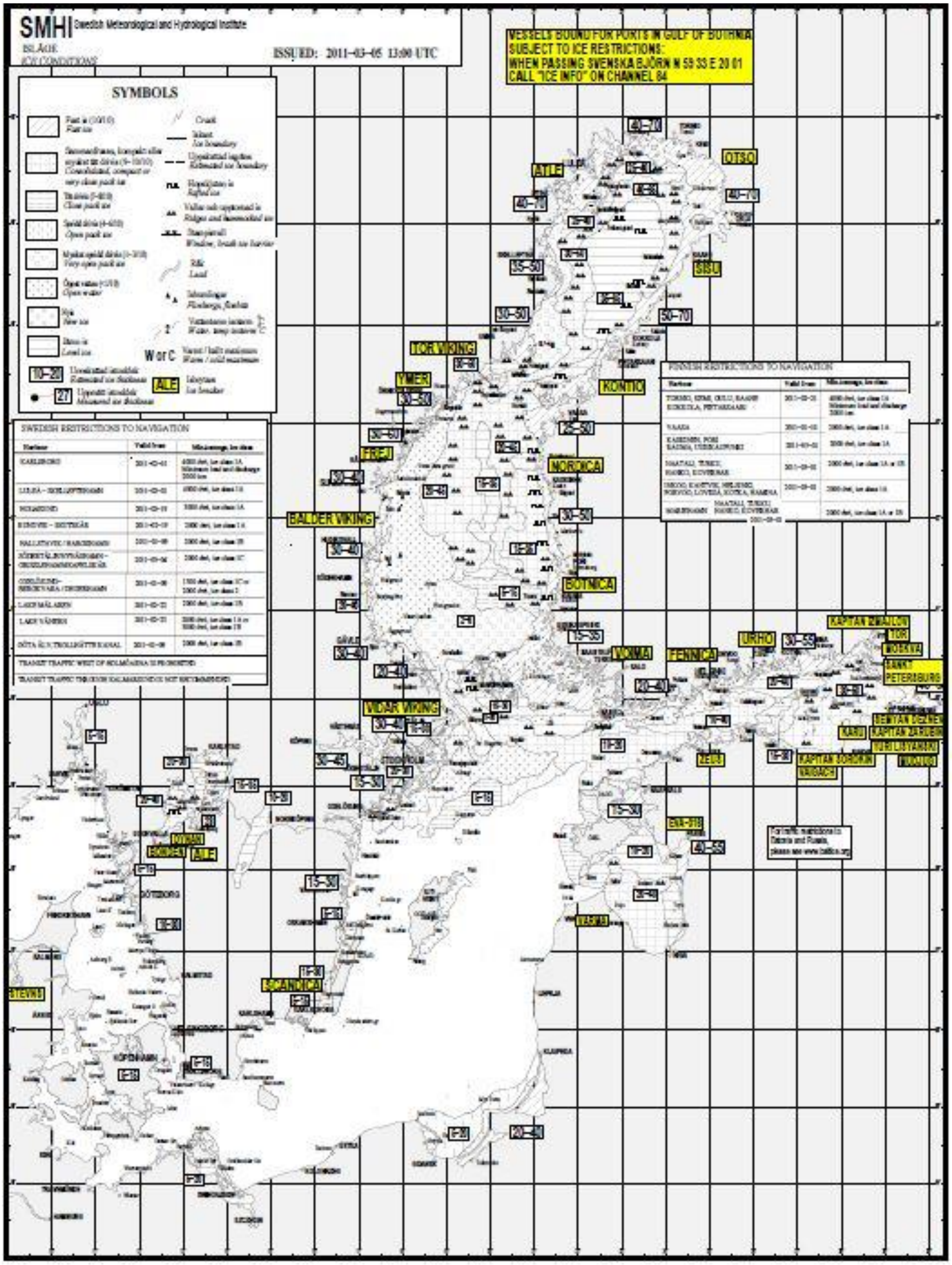

Figure 2.4 The ice chart describing the ice conditions back in 03.05.2011(SMHI).

The easiest way to present the ice conditions in the Baltic Sea is the overview of maximum thickness of undeformed level ice over the whole sea area. The average value of the annual maximum ice thickness in the Baltic can be seen in Figure 2.5. The average annual maximum value of level ice thickness in the northern Baltic is about 70 cm and in the Gulf of Finland about 40 cm. These thicknesses are for the ice cover in the middle of the sea basins, even though the shore-fast ice is usually thicker (Riska, et al., 1997).

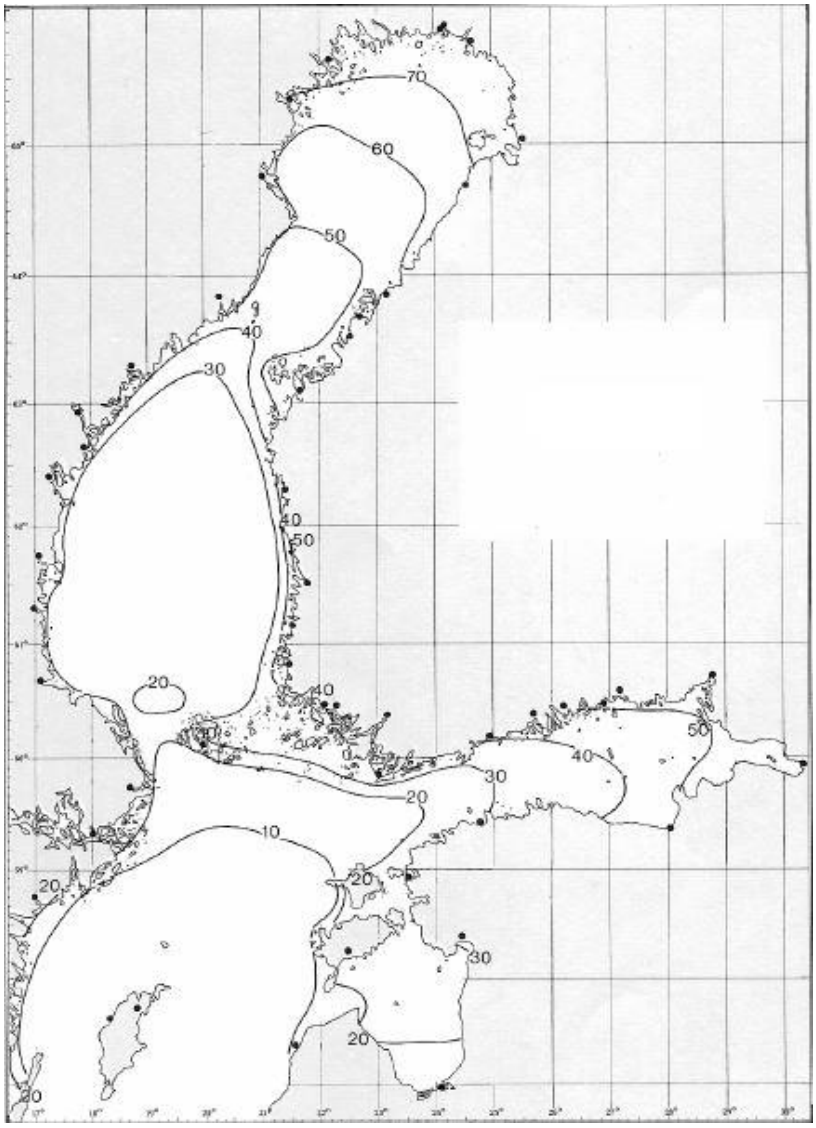

Figure 2.5 The average annual maximum level ice thickness in cm (Riska, et al., 1997).

The salinity of the Baltic Sea is minor comparing to the Atlantic Ocean due to the poor exchange of water with the Atlantic Ocean. Near to the Finnish coast the salinity of the surface water is 3-6 ‰ and in a groundwater 1.4 ‰, whereas in the Atlantic Ocean it is up to 35 ‰. Therefore, the sea water with the normal salinity freezes at temperature of -2 °C and the Baltic Sea at about -0.4 °C (Kujala & Riska, 2010). Thus, this is one reason why ice extent is larger in Baltic Sea than, for instance, in Atlantic Ocean.

Likewise ice thickness, the ice mechanical properties also vary greatly and this is understandable in the case of natural material. Generally, ice mechanical properties are affected by grain size, porosity, salinity and temperature. Therefore, ice cannot be described purely as a brittle, elastic or viscous material. However when designing ice-going vessel, mostly are interested in ice strength values, because based on these values the ice loads are obtained. Therefore, the mean values for the Baltic Sea can be taken the same as Kujala (1994) suggested for the sea ice in the Bay of Bothnia. The average ice characteristic values are presented in Table 2.1.

Table 2.1 Average ice parameters for the Baltic Sea.

Parameter	**Value**	**Unit**
Flexural strength	580	kPa
Crushing strength	2-4	MPa
Density of ice	900	Kg/m^3
Elastic modulus	5	GPa
Porosity	0.3	

During the last decades several methods have been developed for calculating the loads caused by ice-structure impact. Moreover, nowadays there are standards, regulations and guidelines for designing ice-going vessels. The formulas in the previously mentioned rules are often developed in cooperation with classification societies, companies and universities. Therefore, there exists some well-known and a bit less known formulas for calculating the ice load. However, in this particular thesis the most relevant loads are related to level ice. Therefore, some approaches are described in the following sections.

3 METHODS FOR CALCULATING ICE LOADS

3.1 Resistance in level ice

In the Baltic Sea the level ice fields hardly exist and vessels usually operate in the brash ice conditions. They either navigate by their own or they follow the icebreaker in the ice channel by moving in convoy. However, to simplify calculations and model testing the level ice is used as an idealized ice conditions as it gives a first estimation about the load that floating structure experiences.

The average ice force in the time-domain is mainly defined as the ice resistance, and over the years different authors have been proposed several numerical and analytical methods to estimate ship resistance in level ice. However, the most widely used and straightforward method for calculating resistance in level ice was proposed by Lindqvist (1989). To calculate the force for level ice Lindqvist (1989) developed simplified formulas. The total ice resistance during the ice-hull interaction process is divided into three components: ice crushing component, ice breaking component and ice floe submersion component. The model gives resistance as a function of main dimensions, hull form, ice thickness, ice strength and friction. However, based on the collision case investigated in this thesis the Lindqvist model is not suitable to the ship collision with another at a 90 degrees angle in ice, because of the ship's sideways movement after collision with low speed. As a result, the ice breaking process is different from the one adopted by Lindqvist.

3.2 Ice failure mechanics in collision case

In the collision case studied in this thesis, the struck ship after the collision starts to move in sideways. Therefore as was mentioned previously, the ice breaking process is a bit different compared to straightforward ice breaking. Generally, ship breaks ice moving either ahead or astern, and firstly, ice crushing occurs when the contact area is relatively small. During contact area increasing the ice sheet fails in certain stage by bending, because vertical force component

overcomes the bending strength of the ice cover. In other words, ship slides on top of the ice and breaks the ice sheet by its mass. Typical forces during the icebreaking can be seen in Figure 3.1.

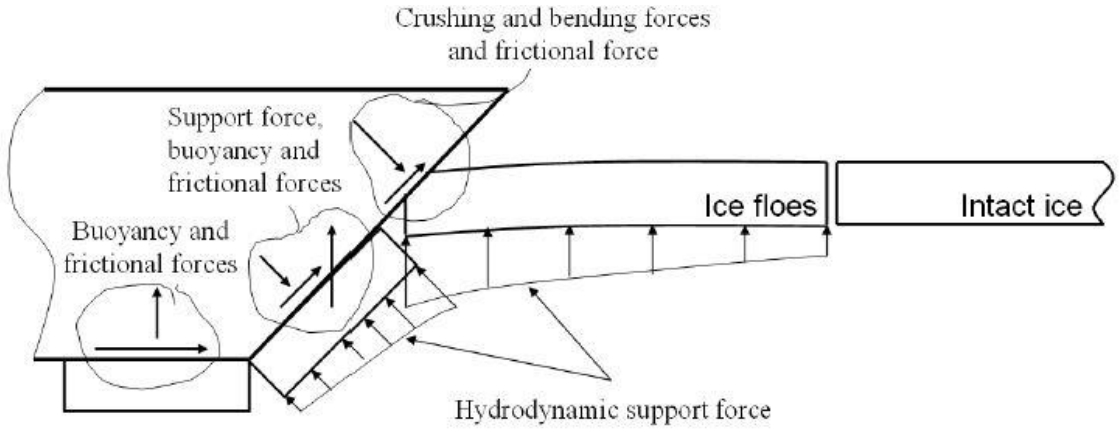

Figure 3.1 The forces in level ice breaking (Riska, 2011).

However, in the case of present collision scenario, the slope angle of side structure is relatively smaller than the bow structures, and therefore, the ice sheet commonly fails due to the crushing. Although, for some ships which have slope angle near to the waterline, bending might occur as well. Nevertheless, it may seem that the breaking process is quite similar, but actually the breaking in sideways is much more complicated due to the long midship area, which causes a great contact area. In addition, the ice floes starts to accumulate, which in turn causes increase in ice loads. There is not available a method for calculating ice force for vessels in such circumstances, but there has been used formulas which are developed for sloping offshore structures (ISO 19906, 2010). In this thesis, it is used formulas that applied Zhou (2012), which similarly to ISO 19906 are based on Croasdale's approach.

3.3 Croasdale's analytical model for calculating ice load

Croasdale (1980) presented a simple elasticity analysis model without rubble effects. The ice sheet was treated as a semi-infinite elastic beam on an elastic foundation subjected to a vertical load P_v and a horizontal load P_h at one end. Furthermore, the method was developed for wide sloping structures and this 2-D approach consists of two processes: the failure of ice sheet by

bending, and riding up/down the sloping surface, depending on the type of structure, either is it upward breaking or downward breaking. The predictive total horizontal ice force per unit meter on the structure is given by

$$q_{Croasdale} = \frac{H}{D} = H_B + H_R \tag{3.1}$$

where D is a width of structure, H_B is breaking force which presents bending failure load and $H_R$is ice ride-up or ride-down force. The equations for these two forces are given as follows:

$$H_B = 0.68 \cdot \xi \cdot \sigma_f \cdot \left(\frac{\rho_w \cdot g \cdot h_i^5}{E}\right)^{1/4} \tag{3.2}$$

and

$$H_R = z \cdot h_i \cdot (\rho_w - \rho_i) \cdot g \cdot (\sin(\alpha) + \mu \cdot \cos(\alpha)) \cdot \\ \cdot \left(\frac{\sin(\alpha) + \mu \cdot \cos(\alpha)}{\cos(\alpha) - \mu \cdot \sin(\alpha)} + \frac{\cos(\alpha)}{\sin(\alpha)}\right) \tag{3.3}$$

where σ_f is the flexural strength of the ice, ρ_w is the density of water, g is acceleration due to the gravity, h_i is the ice thickness, E is the elastic modulus of the ice, z is depth of slope (or draft), ρ_i is the density of ice, μ is the friction coefficient between ice and structure, α is slope angle of the structure and ξ is a function of slope angle and the friction coefficient as given by

$$\xi = \frac{\sin(\alpha) + \mu \cdot \cos(\alpha)}{\cos(\alpha) - \mu \cdot \sin(\alpha)} \tag{3.4}$$

4 MODELLING ICE LOAD FOR A COLLISION SCENARIO

The aim of the thesis was to develop the ice force formula and to investigate the collision energy for certain scenario in ice conditions. Therefore, it is necessary to firstly obtain the ice load which affects the struck ship. Due to the fact that the collision takes place with another ship at a 90 degrees of angle, ice forces applies to the ship side as it moves sideways due to the collision. Thus, the contact length during the ice-structure impact is relatively wide.

Croasdale's 2-D method was chosen to calculate constant horizontal ice load that applies to the ship side. However, Croasdale's method gives result as a load per unit meter. Therefore, it is decided to apply the eq. (4.1), which usually is used to model the line load based on data points. The formula for line load is given as

$$q = C\left(\frac{l_C}{s}\right)^{-a} \tag{4.1}$$

where C and a are unknown parameters, l_C is the contact length and s is the smallest load width, which is typically the value of frame spacing, around 350 mm (Kujala & Arughadhoss, 2012). Generally, the line load curve is provided for illustrative purposes and for comparison to other model tests, observations or numerical methods. However, in this thesis the line load equation has two objectives: to develop constant values for parameters which are unknown, and to calculate the ice forces that affects ship side. Thus, the modification and application of eq. (4.1) is described in later.

During calculation of ice loads it is always necessary to compare obtained results either with model test results, numerically gained results or with experimentally gained data. In this thesis, the comparison and validation is done with experimentally collected and analysed data by Kujala (1991) and with model testing results measured during SAFEWIN project. Kujala (1991) report describes the ice damages of ships, which operated several years in the Northern Baltic. In his study most of the damages appeared at midship area and have occurred while ships have

been stuck in the compressive ice field. Therefore, this experimentally gathered data is valuable to validate the method derived in this thesis. However, the model tests of SAFEWIN project were conducted in the ice basin of Aalto University. How the model test was conducted is described in following sections.

4.1 Model tests

The test program of the SAFEWIN testing included six test series with varying ice thickness and compression levels. The model was fitted with measuring equipment that enabled the registration of resistance, ice loads and ice pressure on the bow shoulder, and the parallel midship during the testing. Furthermore, the force added to the ice sheet by the pusher plates was measured with load sensors on them. The test layout is presented in Figure 4.1.

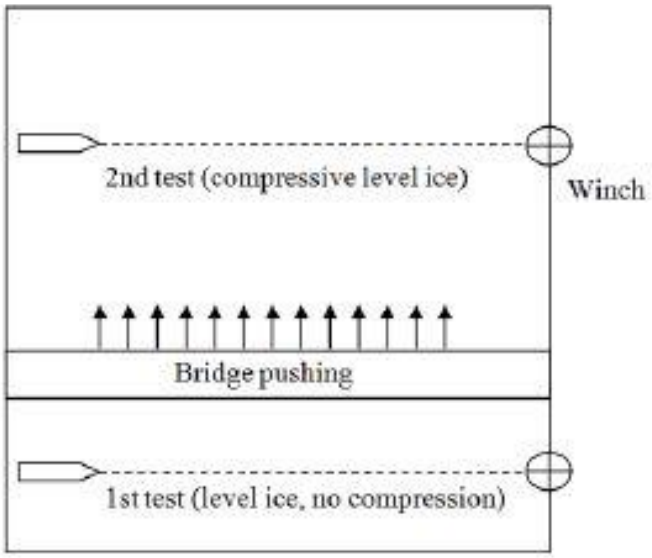

Figure 4.1 Layout of the test arrangement (Suominen & Montewka, 2012).

One of the most important aspect related to the model testing is scaling different properties and parameters. Therefore, always before testing, the model ice properties of each test lane are measured, to verify the suitability for model testing and to obtain a reference to full-scale ice properties. Typical scaling relations for different variables are given in Table 4.1.

Table 4.1 Scaling of different properties in ice model testing (Kujala & Riska, 2010).

		Units			**Units**
Length	$L_{FS} = \lambda \cdot L_M$	m	Ice strength	$\sigma_{FS} = \lambda \cdot \sigma_M$	kPa
Time	$t_{FS} = \lambda^{0.5} \cdot t_M$	s	Ice thickness	$h_{FS} = \lambda \cdot h_M$	m
Velocity	$v_{FS} = \lambda^{0.5} \cdot v_M$	m/s	Elastic modulus	$E_{FS} = \lambda \cdot E_M$	MPa
Force	$F_{FS} = \lambda^3 \cdot F_M$	N	Density	$\rho_{FS} = \rho_M$	kg/m^3
Friction	$\mu_{FS} = \mu_M$	-	Acceleration	$a_{FS} = a_M$	m/s^2

In the Table 4.1 subscript *FS* and *M* denotes for full-scale and model-scale respectively, and λ is a geometric scale factor. The ice properties for different test series during SAFEWIN testing are presented in Table 4.2.

Table 4.2 Ice properties in SAFEWIN testing (Filipović, 2014).

Test series number	**Model scale**				**Ship scale**			
	Thickness [mm]	σ_b [kPa]	σ_c [kPa]	E [MPa]	Thickness [mm]	σ_c [kPa]	σ_b [kPa]	E [MPa]
1	40	30.8	61.5	51	1	1537.5	770	1275
2	29	29.9	50.5	36.75	0.725	1262.5	746.25	918.75
3	23	22.3	74.3	10.4	0.575	1856.5	556.25	260
4	29	29.7	70.7	64.35	0.725	1767.5	741.25	1608.75
5	29	29.5	56.5	65.3	0.725	1412.5	736.25	1632.5
6	24	22.9	69.9	63.15	0.6	1747.5	571.25	1578.75

4.2 Ship model

The SAFEWIN testing was conducted with a 21 300 DWT bulk carrier named Credo model. This certain vessel has an ice class of 1A Super of the Finnish-Swedish Ice Class Rules with a bulbous bow, a high block coefficient and a long parallel midship section. In addition, it should be mentioned that the slope angle for this vessel is a 0 degrees. The scale of the model is 1:25 and the dimensions of the vessel are presented in Table 4.3.

Table 4.3 Dimensions of the vessel (Külaots, 2012).

Parameter	**Full-Scale**	**Unit**	**Model-Scale**	**Unit**
L_{OA}	159	m	6.36	m
L_{PP}	148	m	5.92	m
B	24.6	m	0.984	m
D	13.5	m	0.54	m
T	8.75	m	0.35	m

The model of bulk carrier was prepared without the iceknife, although it actually exists, as can be seen in Figure 4.2.

Figure 4.2 Bulk carrier Credo (Külaots, 2012).

4.3 Ice force calculation model development and validation

SAFEWIN model test results were analysed by Filipović (2014), who used eq. (4.1) to fit curves to the data points of bow shoulder, midship and pusher plates. Based on these fitted curves the unknown parameters, needed for eq. (4.1), were derived for the method developed in this thesis. Additionally, line load curve from ice damage statistics report (Kujala, 1991) was applied for comparison to obtain same load level.

Thus, the idea is firstly to calculate the horizontal ice force by using Croasdale's 2-D method, described in Section 3.3, which gives load as a newton per unit meter. For further steps, this horizontal load is called as the Croasdale's line load. The input values for the calculations were same as was used and measured during SAFEWIN testing, which can be seen in calculations in Appendix 1. However, the slope angle was chosen to be 1 degree instead 0 degrees. The reasons for this will be discussed later in this work. Despite of the rather vertical hull side, it is still assumed that the ice sheet bends during the impact, so the Croasdale's approach could be applied. Croasdale's line load was calculated for three different cases where ice thicknesses were following: 40 *mm*, 29 *mm* and 24 *mm*. According to this, it is possible to compare how ice

thickness affects the line load, which in turn, has also influence on choosing a constant parameter for contact length l_C. However, respectively to bulk carrier Credo line load curves (Filipović, 2014), the obtained line load from Croasdale's method was marked in the Credo's line load graph based on its value, see Figure 4.3. The Croasdale's line load value for different thicknesses varied from 55 to 93 *N/m.*

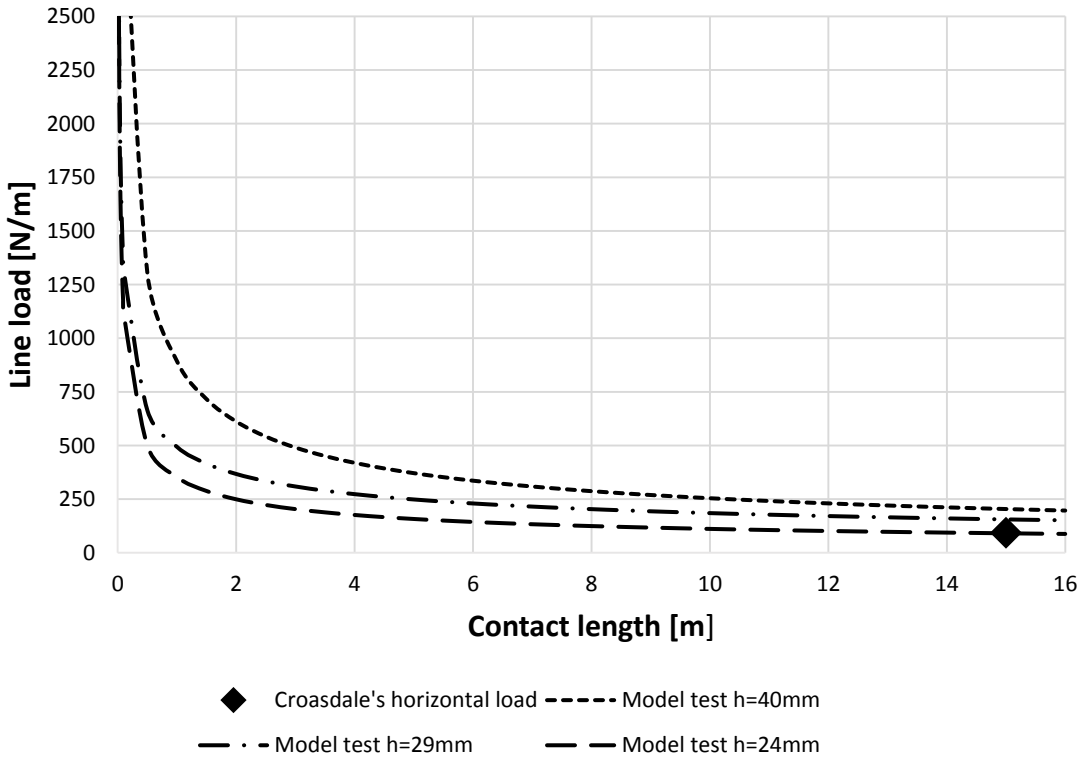

Figure 4.3 Calculated Croasdale's horizontal load and fitted line load curves for different thicknesses (Filipović, 2014).

From the graph it is obtained the contact length l_C, based on the Croasdale's line load which is near to the results from Credo's model testing. Therefore, the contact length was chosen to be 15 *m*. This contact length was chosen as small as possible, so it would qualify for small slope angles and for greater angles as well. Further, it can be clearly seen that, when contact length decreases, the line load increases. Therefore for wide structures, the line load is minor comparing to, for example, some certain region on ship side where the contact length is small.

Next, the line load curve presented by Kujala (1991) is applied to verify that derived ice force formula will give a result as close as possible to actual ice loads that was experimentally measured. Therefore, as the contact length l_C is known it is possible to derive parameter C value from line load equation, where s is typically known as frame spacing and exponent a is taken as -0.71, based on Kujala (1991) report. However, the Croasdale's line load is added to the derivation as can be seen as follows:

$$q = C \cdot \left(\frac{l_C}{s}\right)^{-a} \Rightarrow C = \frac{q_{Crosadale}}{\left(\frac{l_C}{s}\right)^{-a}} \tag{4.2}$$

After the parameter C value was calculated, based on the Croasdale's line load value, all the unknown parameters were received for further calculations to obtain line load graph. Therefore, the line load can be calculated by applying the actual considered contact length L_{mid} :

$$q = C \cdot \left(\frac{L_{mid}}{s}\right)^{-a} = \frac{q_{Crosadale}}{\left(\frac{l_C}{s}\right)^{-a}} \cdot \left(\frac{L_{mid}}{s}\right)^{-a} \tag{4.3}$$

As the line load equation is derived, it is compared with the line load curve proposed by Kujala (1991). The ice properties used in this calculation are same as presented in Table 2.1 in Section 2.2, see also in Appendix 1. Kujala study was conducted with many ships, and therefore, the height from the waterline to the bottom of structure was assumed as 9.2 *m* and ice thickness was taken as 0.7 *m.* The Figure 4.4 shows that the derived initial formula underestimates the actual situation, therefore eq. (4.3) is multiplied with the coefficient 2.6 which will give similar line load curve as given in Kujala report. As a result of that the method is valid and it will give the same load level as in real ice conditions.

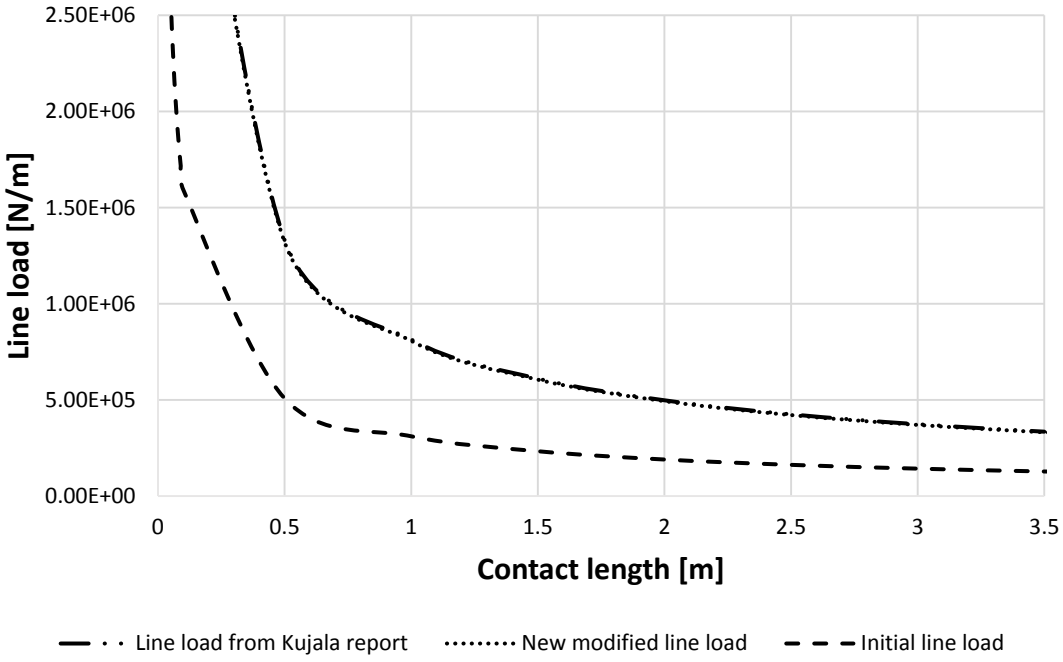

Figure 4.4 Line load curve comparison with curve obtained by Kujala (1991).

Thus the new formula for line load is given as follows:

$$q = C \cdot \left(\frac{L_{mid}}{s}\right)^{-a} \cdot 2.6 = \frac{q_{Crosadale}}{\left(\frac{l_C}{s}\right)^{-a}} \cdot \left(\frac{L_{mid}}{s}\right)^{-a} \cdot 2.6 \tag{4.4}$$

Further, it is possible to derive the final ice force formula, based on the actual contact length/midship length. Thus, the ice force for sideways moving ship is calculated as follows:

$$F_{ice} = q \cdot L_{mid} \cdot 2.6 = \frac{q_{Crosadale}}{\left(\frac{l_C}{s}\right)^{-a}} \cdot \left(\frac{L_{mid}}{s}\right)^{-a} \cdot L_{mid} \cdot 2.6 \tag{4.5}$$

All the line load calculations can be seen in Appendix 1. In accordance with the eq. (4.4) the calculation model results are compared with the fitted curves presented by Filipović (2014). The comparison of the line load curves are presented in Figure 4.5, Figure 4.6 and in Figure 4.7.

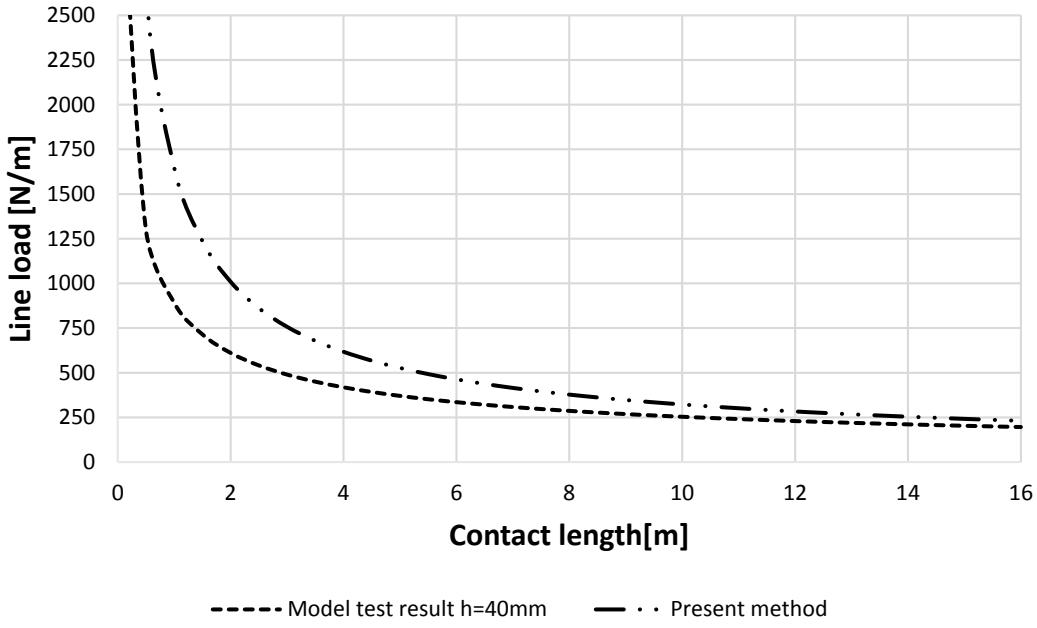

Figure 4.5 Line load curves if ice thickness is 40 mm.

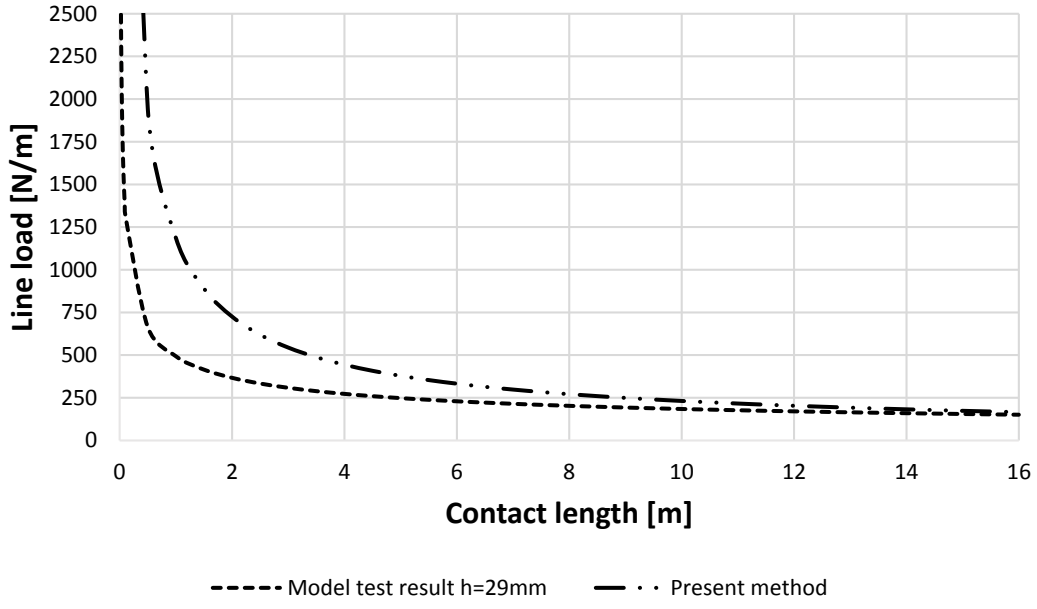

Figure 4.6 Line load curves if ice thickness is 29 mm.

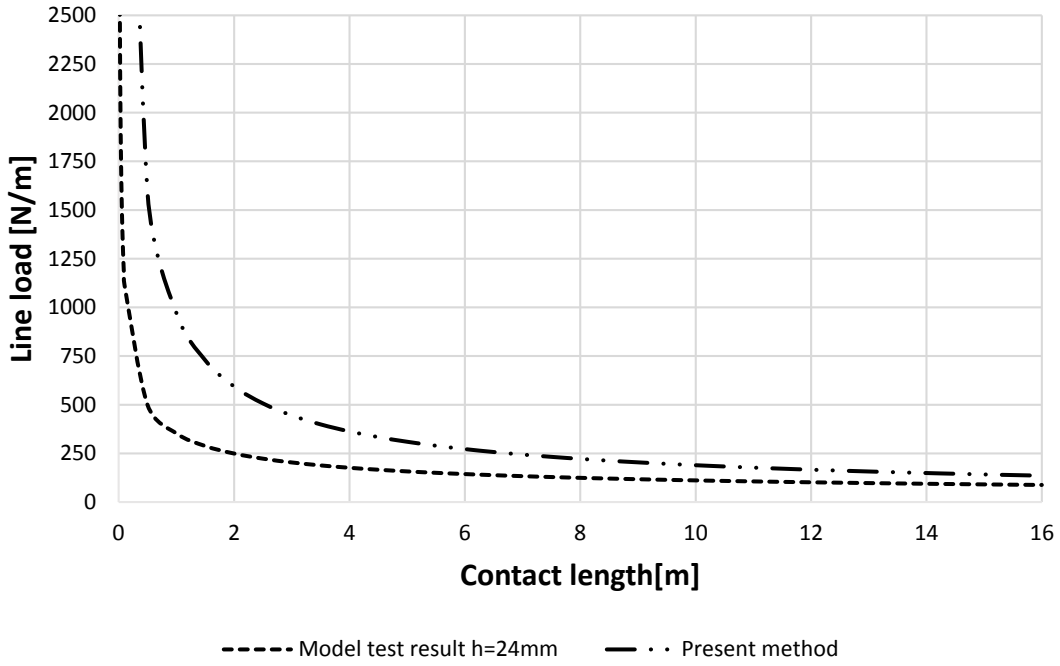

Figure 4.7 Line load curves if ice thickness is 24 mm.

Based on the comparison in these figures it is well identified that the fitting of the curves gets better if the contact length increases. Additionally, multiplying with the coefficient 2.6 justified itself as the agreement is better than it would be without the coefficient. However, it must be taken into account that for a smaller contact length the ice load may be overestimated. Although, it should be remembered that model ice characteristics may vary also from the real conditions.

One of the reason for the difference in fitting is the selection of the contact length, which is chosen to be constantly 15 *m*. In fact, for the higher contact length values, the variation of the line load is smaller. Hence, this contact length was chosen in a way that it would be suitable whatever case, so it would give approximately the same result with the actual load.

Another, and probably the biggest reason for the variation in the fitting, is the slope angle chosen for this certain case. Croasdales's method is developed for sloping structures where the slope angle of the structure is typically in range of 45° to 60°. Therefore, the ice failure process can be easily allocate as a crushing failure and bending failure. In this thesis the crushing failure is not considered. However for the vessels, the slope angle of the side structure beneath the waterline can be approximately 10°, although for most cargo ships and tankers the slope angle

is almost near to zero degrees. This is the reason why the ice failure modes during vessel's sideways movement is mixed process, and it is relatively complicated to distinguish the exact ice failing mode. Nevertheless, it is proved that the Croasdales's method is suitable to calculate the ice loads to ship side when the slope angle is approximately 9° (Zhou, et al., 2012). Thus, it can be seen from the present work the method suits also fairly well for very small slope angles, based on the comparison with SAFEWIN project model testing results. Despite of the results agreement, the sensitivity of slope angle to the contact length in range of 0.1 to 1 degrees is great, as can be seen from Figure 4.8. However, as can be seen for the further increase of the slope angle, the contact length increase was not necessary as the results fitted well comparing to line loads from model testing. Therefore, due to the sake of simplicity it has been decided to apply 1° in the calculations for the vessels where slope angle is actually near to the zero degrees. Based on that, it is possible to take the preliminary contact length 15 *m* for calculating *C* parameter. For the higher than 1 degree of slope angle, the change of contact length does not affect the line load so much anymore, so it can be taken as constant. However, it should be mentioned that 15 *m* contact length is only used for calculating parameter C, but the developed ice line load formula allows to obtain ice load for contact length which are interested in.

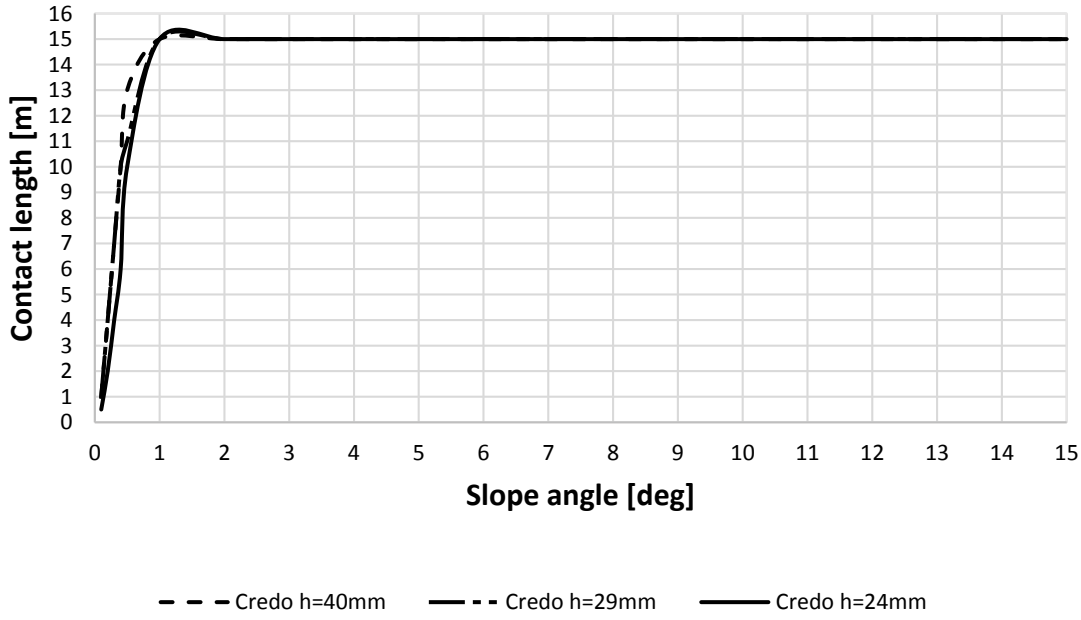

Figure 4.8 Contact length dependence on slope angle.

As a result, a method is developed which evaluates ice loads to the ship which moves in sideways because of the collision at a 90 degree angle with another ship. The method showed satisfactory agreement with the results of SAFEWIN model testing and will be used for further collision calculations in ice to estimate deformation energy.

5 SHIP-SHIP-ICE COLLISION SIMULATION MODELS

In the last decade marine traffic has increased significantly in the Baltic Sea, which in turn, leads to the greater risk of ship collisions. Therefore, investigating ships crashworthiness in collision accident is highly essential, to prevent the environmental damage.

The first models for analyzing ship collisions were developed in 1950s, which were for nuclear powered ships, and henceforward can be applied mainly for tankers and LPG/LNG carriers. Typically, collision analysis models consists of external ship dynamics and inner mechanics. However, nowadays collision models use different sub-models and simulation or coupling approaches (Chen, 2000). Therefore, two different approaches for collision calculation are described in following sections: a model based on momentum conservation allowing easy estimation of ice effects and time-domain collision simulation model allowing more precise evaluation.

5.1 Simulation model based on the conservation of momentum

Earlier collision models, such as by Minorsky (1959) are based on the conservation of momentum. The law of conservation of momentum states that the total momentum of isolated system before collision is always equal to total momentum after the collision. The principle of the conservation of momentum in ship collision analysis was firstly used by Minorsky (1959), who was primarily concerned about crashworthiness of the nuclear powered ships in right angle collision. Minorsky approach is based on the following assumptions:

- The collision is totally inelastic.
- The system kinetic energy along the struck ship's longitudinal direction is negligible.
- The rotation of the struck and striking ships are small and can be neglected.

The first two assumptions define the so-called "worst case". The third is based on the observation of only small rotations in actual collisions during the damage event. Small rotations have also been observed in theoretical analysis.

Based on these assumptions, the system becomes simple one dimensional problem and the final velocities of both striking and struck ships can be derived on the basis of conservation of momentum:

$$(M_A + M_B + dm)V_{com} = M_A V_A \,, \tag{5.1}$$

and

$$V_{com} = \frac{M_A V_A}{(M_A + M_B + dm)}, \tag{5.2}$$

where M_A is mass of striking ship, M_B is mass of struck ship, dm is added mass of struck ship in the sway direction, V_{com} is final common velocity in the direction of striking vessel, normal to the struck ship's centreline and V_A is initial velocity of the striking ship in Y direction.

The kinetic energy lost in the collision is the difference between initial kinetic energy and the final kinetic energy remaining in the system after impact. Thus, the total kinetic energy absorbed in the collision is then:

$$\Delta KE = \frac{1}{2} M_A V_A^2 - \frac{1}{2}(M_A + M_B + dm)V_{com}^2 = \frac{1}{2}\frac{M_A(M_B + dm)}{(M_A + M_B + dm)} V_A^2 \,. \tag{5.3}$$

The virtual added mass of liquid, dm, in the case of a hull vibrating transversally in deep water, was estimated to be taken approximately as $0.4M_B$. Nowadays, more precise estimation for virtual mass can be obtained via different calculation approaches such as strip-theory for example. The collision angle ϕ, is introduced to calculate the velocity of the striking ship in the sway direction of the struck ship. The absorbed kinetic energy in the struck ship transverse direction is:

$$\Delta KE = \frac{M_A M_B}{2M_B + 1.43M_A}(V_A sin\phi)^2 \,, \tag{5.4}$$

where V_A is the initial velocity of the striking ship.

However, this model has been modified and extended up to three degree-of-freedom in horizontal plane by Zhang (1999).

Present thesis aims to include ice in the collision dynamics. Therefore, it is necessary to add equivalent ice mass M_{ice} to eq. (5.1) to yield to proper loss of kinetic energy. Thus, the lost kinetic energy or in other words deformation energy of struck ship is calculated by using the following formula:

$$E_{Def} = \frac{1}{2}\frac{M_A(M_B + dm + M_{ice})}{(M_A + M_B + dm + M_{ice})}V_A^2. \tag{5.5}$$

Definition of M_{ice} is not trivial and an approach to define it is proposed here. The definition is based on the establishment of energy balance in collision. The energy balance can be written as:

$$E_0 = E_{Def} + E_{K,A} + E_{K,B} + E_{ice}, \tag{5.6}$$

where E_0 is total kinetic energy before collision, E_{Def} is lost kinetic energy, or in present context deformation energy, $E_{K,A}$ is striking ship kinetic energy after collision, $E_{K,B}$ is struck ship kinetic energy after collision and E_{ice} is kinetic energy that is absorbed by ice.

Energy balance equation can be written also as follows:

$$\frac{M_A \cdot V_A^2}{2} = \frac{1}{2}\frac{M_A(M_B + dm + M_{ice})}{(M_A + M_B + dm + M_{ice})} \cdot V_A^2 + \frac{M_A \cdot V_{com}^2}{2} + \\ + \frac{M_B \cdot V_{com}^2}{2} + F_{ice} \cdot x_B, \tag{5.7}$$

where F_{ice} is ice force, calculated with eq. (4.5) in Section 4.3, x_B is a struck ship displacement after collision, M_{ice} is ice mass and V_{com} is the final common velocity, that is given as:

$$V_{com} = \frac{M_A V_A}{(M_A + M_B + dm + M_{ice})}. \tag{5.8}$$

In order to obtain struck ship displacement, it will be approximated from the following formula:

$$x_B = V_B \cdot t_{com} = \frac{V_{com}}{2} \cdot t_{com}\,, \tag{5.9}$$

where t_{com} is the time when ships reach to the common velocity V_{com}. However, struck ship displacement can be written also based on the knowledge that the penetration depth δ is a difference between the displacements of the striking ship and the struck ship:

$$x_B = -\delta + x_A \,, \tag{5.10}$$

where striking ship displacement x_A is calculated as follows:

$$x_A = \left(V_A - \frac{V_{com}}{2}\right) \cdot t_{com} \,. \tag{5.11}$$

As was described above, penetration depth can be written based on the eq. (5.9) and (5.11):

$$\delta = \left(V_A - \frac{V_{com}}{2}\right) \cdot t_{com} - \frac{V_{com}}{2} \cdot t_{com} = \ (V_A - V_{com}) \cdot t_{com}. \tag{5.12}$$

In this derivation we assume a constant velocity, even though during collision process the ship velocities are obviously changing. However, the main aim here is to obtain only the final common velocity which is calculated based on masses and initial speed in eq. (5.8).

Another way the penetration depth can be calculated is from a simplified deformation energy eq. (5.13) where is assumed stiffness k is increasing linearly, where stiffness is characteristics of structure which indicates its rigidity.

$$E_{Def} = \frac{F_c \cdot \delta}{2} \tag{5.13}$$

In eq. (5.13), F_c is collision force which is a linear function of ship stiffness k and penetration depth δ:

$$F_c = k \cdot \delta. \tag{5.14}$$

Therefore, from eq. (5.13) and eq. (5.14) it is possible to state that δ is:

$$\delta = \sqrt{\frac{E_{Def} \cdot 2}{k}}. \tag{5.15}$$

Based on that, equalizing eq. (5.12) and (5.15), t_{com} can be defined as follows:

$$\begin{aligned} &(V_A - V_{com}) \cdot t_{com} = \sqrt{\frac{E_{Def} \cdot 2}{k}} \;\Rightarrow \\ &t_{com} = \frac{\sqrt{\frac{E_{Def} \cdot 2}{k}}}{(V_A - V_{com})} = \frac{\sqrt{\frac{E_{Def} \cdot 2}{k}}}{\left(V_A - \frac{M_A V_A}{(M_A + M_B + dm + M_{ice})}\right)}. \end{aligned} \tag{5.16}$$

Further, the struck ship displacement can be written based on eq. (5.11), (5.15) and (5.16) as

$$\begin{aligned} x_B = -\delta + x_A &= -\sqrt{\frac{E_{Def} \cdot 2}{k}} + \left(V_A - \frac{V_{com}}{2}\right) \cdot t_{com} \\ &= -\sqrt{\frac{E_{Def} \cdot 2}{k}} + \left(V_A - \frac{M_A V_A}{2(M_A + M_B + dm + M_{ice})}\right) \\ &\cdot \frac{\sqrt{\frac{E_{Def} \cdot 2}{k}}}{\left(V_A - \frac{M_A V_A}{(M_A + M_B + dm + M_{ice})}\right)}, \end{aligned} \tag{5.17}$$

which after simplifying can be written as follows:

$$x_B = \frac{M_A \sqrt{\frac{E_{Def} \cdot 2}{k}}}{2(M_B + dm + M_{ice})}. \tag{5.18}$$

Finally, substituting eq. (5.18) to eq. (5.7), the energy balance is obtained as:

$$\frac{M_A \cdot V_A^2}{2} = \frac{1}{2} \frac{M_A (M_B + dm + M_{ice})}{(M_A + M_B + dm + M_{ice})} \cdot V_A^2 + \frac{M_A \cdot V_{com}^2}{2} + \tag{5.19}$$

$$+\frac{M_B \cdot V_{com}^2}{2} + F_{ice} \cdot \frac{M_A\sqrt{\frac{E_{Def} \cdot 2}{k}}}{2(M_B + dm + M_{ice})},$$

From this equation the equivalent ice mass M_{ice} can numerically be obtained with the help of mathematical software. It should be mentioned that the final mathematical form of M_{ice} is cumbersome and too long to present here. It provides three possible solutions, out of which the only positive value presents the correct value for M_{ice}. The ice mass value derived from eq. (5.19) can be used with the deformation energy formulation, eq.(5.5), to give the deformation energy that considers the influence of the sheet ice.

5.2 Time-domain simulation model

Although the conservation of momentum approach gives a deformation energy estimation quite quickly, it does not provide usually result as accurate as the time-domain model. In this section, the time-domain simulation model is described based on Tabri (2010).

A time domain simulation of collision considers inertial forces, hydrodynamic forces and hydrostatic force in a single calculation, and gives ships' behaviour with the collision forces. In this case, also ice force, which calculation was described in Section 4.3 is added to the calculation. The relation between the forces and the ship motions is described through a system of equations of motion for each ship. The contact force is derived with the help of a kinematic condition based on the relative motion between the ships.

The time integration of the equations of motion is based on an explicit 5th –order Dormand-Price integration scheme, which is a member of the Runge-Kutta family solvers. Inside a time integration increment, seven sub-increments are calculated. The hydrodynamic inertia force, the restoring force, the ice force calculated with eq. (4.5), and the ship motions are updated in every sub-increment. On the other hand, the contact force, velocity-dependent radiation force, and the hydrodynamic drag are kept constant during the whole integration increment for the sake of time efficiency.

The procedure of the time domain simulation is divided into three steps. First, at time t, the position, velocity, and acceleration are known for both ships. Secondly, the external forces are calculated for time t on the basis of these values. The gravity force is constant throughout the collision and acts along the global vertical axis z^0. The hydromechanical forces are calculated in a local coordinate system from the position and motions of the ships.

For the contact force the relative position and motions are presented in the local coordinate system of the striking ship, where the contact force is calculated. Finally, the values of the initial parameters are all substituted into equations of motion, wherefrom the values of the ship motions are solved for time instant $t + \Delta t$.

The solution of the equations of motion for both colliding ships at time instant $t + \Delta t$ provides kinematically admissible motions given in the local coordinate systems of ships. The new position of the ship's centre of gravity at $t + \Delta t$ with respect to the inertial frame is evaluated by transforming the translational displacement increments to the inertial frame. After this, the orientation with respect to inertial frame is updated by the angular increments of Euler's angles. The process is repeated until the end of the collision.

6 COLLISION DYNAMICS IN ICE AND IN OPEN WATER

In this chapter is analysed and described collision calculations in open water and in ice. The open water results are calculated with Tabri's time-domain model and with Minorsky's model based on conservation of momentum. The ice collision calculation are done with Tabri's time-domain model considering developed ice force formula.

For calculations few more parameters needs to be considered. During the impact, ice structure interaction takes place. Therefore, the friction coefficient must be considered. Previously in ice force formula development, coefficient was taken from model tests. In following is proposed friction coefficient for collision calculations. Lindqvist (1989) suggested the value for the friction coefficient between average ship with anti-fouling paint and the sea ice to be around 0.15. The Finnish-Swedish ice class rules suggest the friction coefficient to be at the range of 0.05 for new ships to 0.15 for a corroded hull surface. Based on these references, 0.1 is applied as it seems to be reasonable for average ships in the Baltic Sea. In addition it is assumed that struck ship sway added mass is $0.47M_B$ and striking ship surge added mass is $0.05M_A$.

The results of collision calculation is based on the case where tanker with length of 190 meters strikes another tanker with length of 150 meters. Striking velocity is 3 *m/s*, stiffness k is 7.29E+06 *N/m* and the ice thickness was chosen to be 1.5 meters. The ice load for this case is 7.21E+06 *N*.

Calculation results are presented in the figures below. As a result of contact between the ships the speed of the striking ship reduces rapidly while the struck ship accelerates, see Figure 6.1. The ships separate and the contact force reduces to zero, see Figure 6.2. However, due to the higher hydrodynamic resistance of struck ship and partly also due to the presence of ice, a second contact takes place as well. However, the second force peaks does not influence the maximum penetration depth, see Figure 6.4. Influence of the force peaks is clearly seen also in the accelerations in Figure 6.3. In Figure 6.4 the linear dependence between the contact force

and penetration depth can be observed and the maximum penetration is achieved once the velocities of both ships have equalized and reached to V_{com}.

a) b)

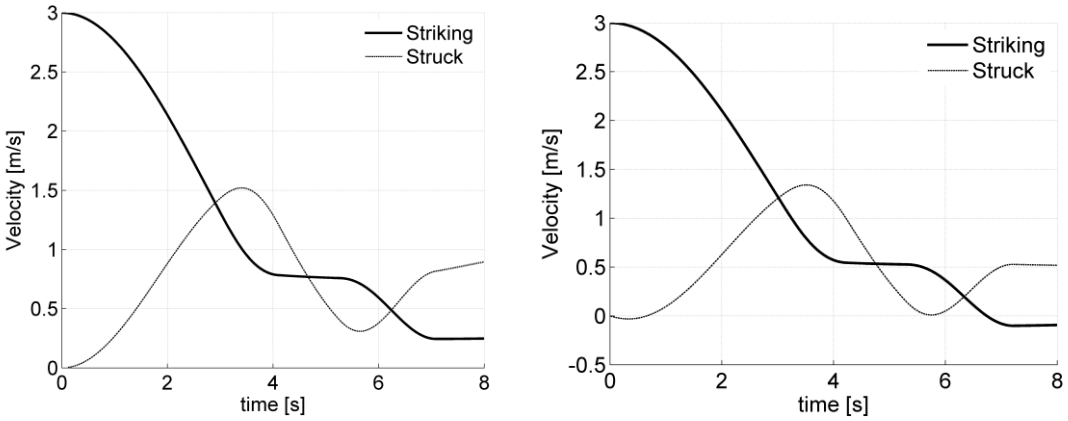

Figure 6.1 Velocities as a function of time of striking and struck ship in a) open water and b) in 1.5 m thick ice.

a) b)

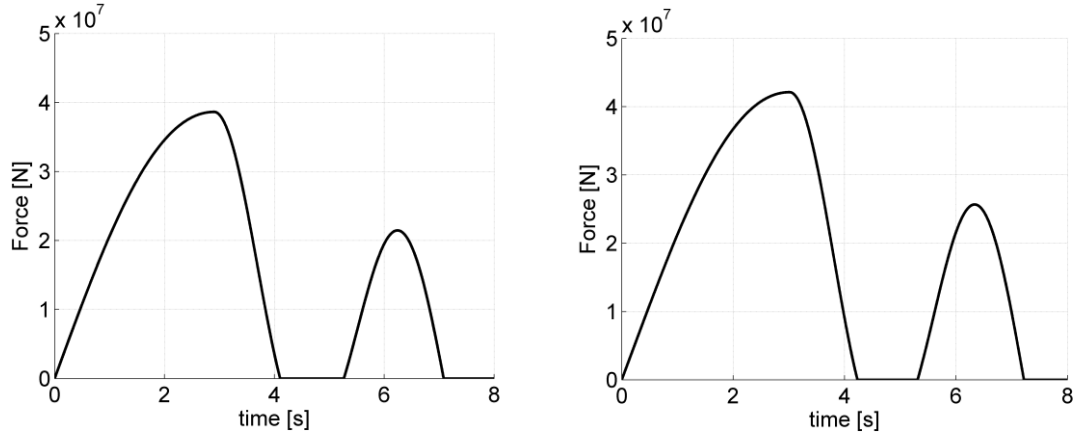

Figure 6.2 Collision force as a function of time in a) open water and b) in 1.5 m thick ice.

a) b)

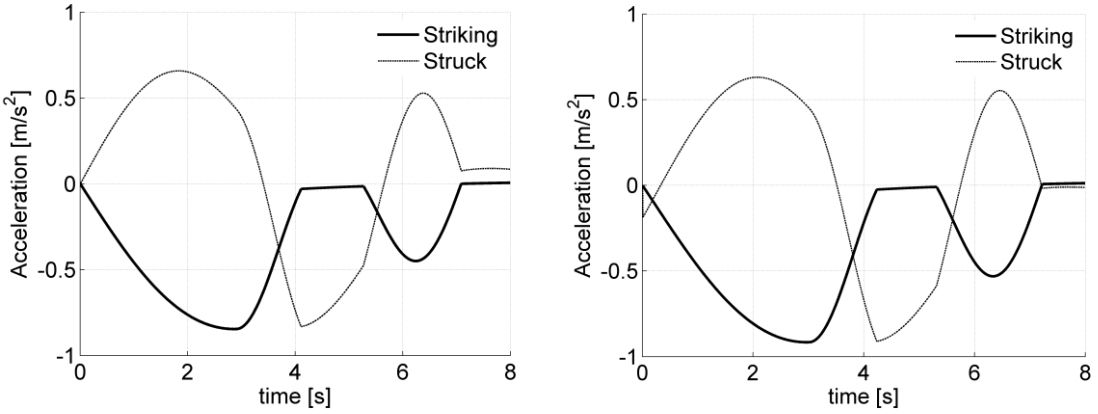

Figure 6.3 Acceleration as a function of time of striking and struck ship a) in open water and b) in 1.5 m thick ice.

a) b)

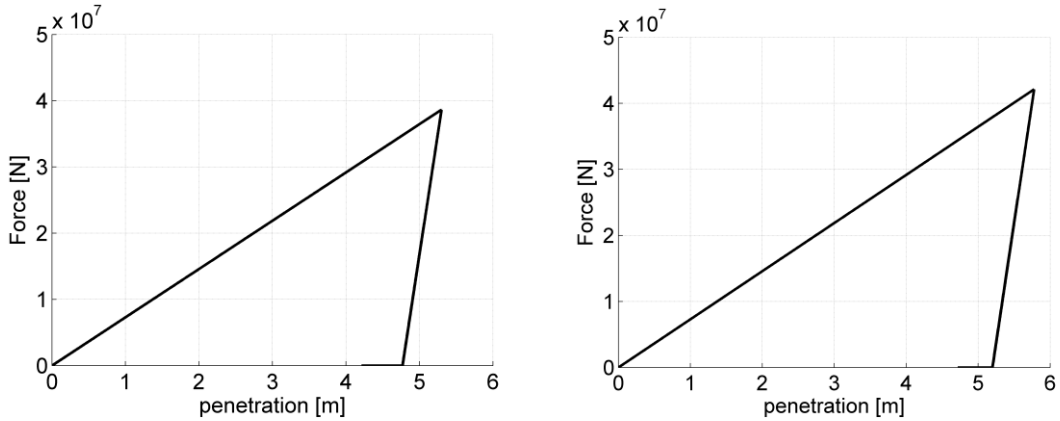

Figure 6.4 Collision force as a function of penetration a) in open water and b) in 1.5 m thick ice.

The difference in between the penetration in open water and in ice is approximately 0.5 *m*, see Figure 6.4. In addition, the agreement comparing to the time domain model and derived simplified model is great as the difference in penetration is only 0.04 *m*.

If comparing the different simulations, the contact force is only slightly higher for the case with ice thickness of 1.5 *m*, see Figure 6.4. The same phenomena can be observed from energy balance in Figure 6.5. The figure reveals that the presence of ice only slightly increases the deformation energy, while the importance of energy absorbed by ice is small compared to other

energy absorbing mechanisms. Note also that most of the energy is absorbed before the ships reach to common velocity, which is approximately at 3.5 seconds. The small influence of rather thick ice sheet indicates that the ice force calculated with present approach are small compared to other force components, mainly the contact force and the inertial forces.

a) b)

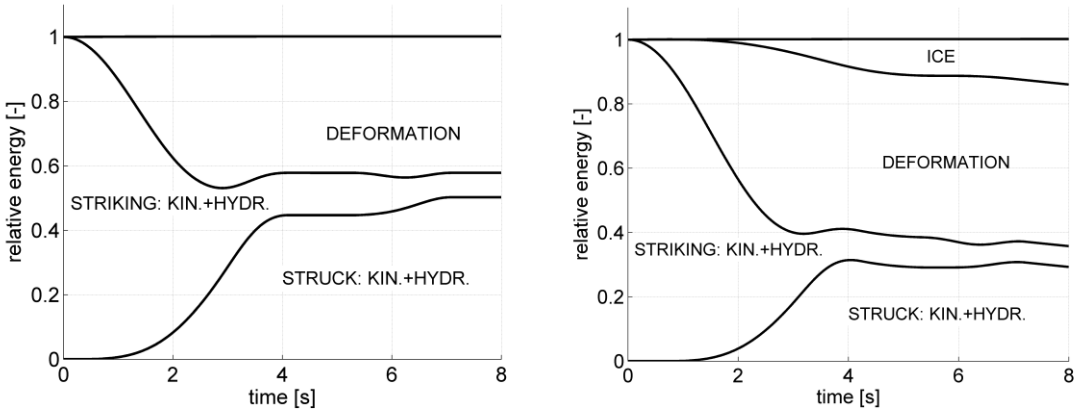

Figure 6.5 Relative energy components throughout the collision a) in open water and b) in 1.5 m thick ice

Finally, Figure 6.6a presents the relationship of time-domain model and Minorsky's momentum of conservation, both calculated in open water. Figure 6.6b presents the relationship where ice is included only to time-domain model. Figures indicates clearly the model based on momentum of conservation calculates constant value, whereas the time-domain evaluates the whole process in time domain. Similarly to the force-penetration curve, the maximum penetration is reached when deformation energy is maximum. The deformation energy obtained in ice in this certain collision scenario is 19% greater than the outcome reached in open water by using time-domain model. If comparing simplified model result in 1.5 *m* thick ice, the difference is only approximately 1% in this case.

a) b)

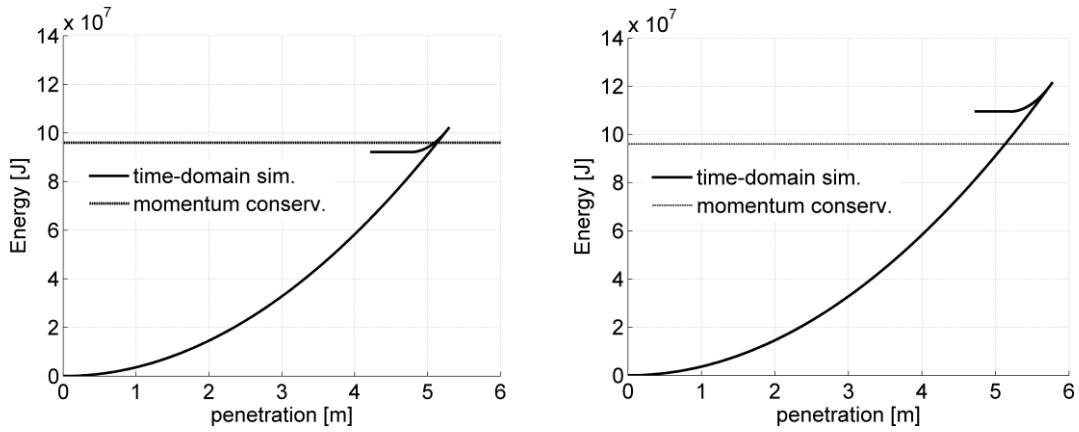

Figure 6.6 Energy as a function of penetration a) in open water and b) in 1.5 m thick ice.

7 PARAMETRIC STUDY

A parametric study has been conducted to present the influence of different parameters. A right angle collisions were simulated by using four different size tankers. The ships parameters are presented in Table 7.1. In all the scenarios the struck ship is 150 *m* long tanker and the striking ship varies to study the influence of deformation energy and penetration depth on the mass of the striking ship. In Table 7.1 is also presented the ice loads calculated with eq.(4.5), that affects struck ship. That struck ship is initially motionless and the striking ship velocity is 3, 6 or 9 *m/s*. Thus, in total 48 scenarios are simulated with each stiffness value. Two different stiffness's of ship structure are studied.

Table 7.1 General dimensions of ships involved in collision scenarios and ice load based on ice thickness for struck ship T150.

Ship	**L [m]**	**B [m]**	**T [m]**	C_B	**Mass [kg]**	**Ice thickness [m]**	**Ice load [N]**
Tanker T120	120	16	8	0.8	1.29E+07	**0**	0
Tanker T150	150	24	9	0.9	2.08E+07	**0.5**	2.39E+06
Tanker T190	190	24	12	0.8	4.61 E+07	**1**	4.80E+06
Tanker T235	235	32	18	0.8	1.14 E+08	**1.5**	7.21E+06

7.1 Collision in open water

Open water collisions have been simulated and calculated already by several different researchers with different methods. Therefore, it is possible to calculate collision in open water relatively easily, for example, using the law of conservation of momentum. Currently there does

not exist any certain method to evaluate deformation energy of struck ship due to collision in ice. Hence, validating the method developed in this thesis is difficult as there is no other similar approaches for comparison. However, comparing outcome in ice conditions with the open water results, helps to give a qualitative understanding on the influence of ice on ship collision dynamics. Due to the extra mass coming from ice, the deformation energy should increase and the penetration depth has to be greater. Open water results were obtained by using time-domain calculation model (Tabri, 2010) and method based on the conservation of momentum (Minorsky, 1959).

Calculations based on the conservation of momentum are quite straightforward, while time-domain needs some more complicated formulas and additional input parameters for calculations. One of the parameter, which affects calculations remarkably is stiffness of the ships structure. The values of stiffness are chosen based on a former study, which was not part of this thesis. To study the influence of stiffness, two different values were used in the analysis: 1.46E+07 *N/m* and 7.29E+06 *N/m*. The results of open water collision can be seen in Table 7.2 and in Table 7.3

Table 7.2 Result of collisions in open water when k is 1.46E+07 N/m.

Striking-Struck	Striking ship mass [kg]	Struck ship mass [kg]	Striking speed [m/s]	Transverse penetration with time-domain model [m]	Def. energy with time-domain model [J]	Def. energy with Minorsky's model [J]
T120-T150	1.29E+07	2.80E+07	3	2.49	4.52E+07	4.51E+07
	1.29E+07	2.80E+07	6	4.98	1.81E+08	1.80E+08
	1.29E+07	2.80E+07	9	7.47	4.07E+08	4.06E+08
T150-T150	2.80E+07	2.80E+07	3	3.19	7.44E+07	7.46E+07
	2.80E+07	2.80E+07	6	6.39	2.98E+08	2.99E+08
	2.80E+07	2.80E+07	9	9.60	6.71E+08	6.72E+08
T190-T150	4.61E+07	2.80E+07	3	3.69	9.95E+07	9.60E+07
	4.61E+07	2.80E+07	6	7.40	3.99E+08	3.84E+08
	4.61E+07	2.80E+07	9	11.12	9.02E+08	8.64E+08
T235-T150	1.14E+08	2.80E+07	3	4.40	1.41E+08	1.30E+08
	1.14E+08	2.80E+07	6	8.83	5.69E+08	5.21E+08
	1.14E+08	2.80E+07	9	13.31	1.29E+09	1.17E+09

Table 7.3 Result of the collision in open water when k is 7.29E+06 N/m.

Striking-Struck	Striking ship mass [kg]	Struck ship mass [kg]	Striking speed [m/s]	Transverse penetration with time-domain model [m]	Def. energy with time-domain model [J]	Def. energy with Minorsky's model [J]
T120-T150	1.29E+07	2.80E+07	3	3.51	4.50E+07	4.51E+07
	1.29E+07	2.80E+07	6	7.03	1.80E+08	1.80E+08
	1.29E+07	2.80E+07	9	10.54	4.05E+08	4.06E+08
T150-T150	2.80E+07	2.80E+07	3	4.50	7.40E+07	7.46E+07
	2.80E+07	2.80E+07	6	9.02	2.97E+08	2.99E+08
	2.80E+07	2.80E+07	9	13.54	6.69E+08	6.72E+08
T190-T150	4.61E+07	2.80E+07	3	5.30	1.02E+08	9.60E+07
	4.61E+07	2.80E+07	6	10.63	4.12E+08	3.84E+08
	4.61E+07	2.80E+07	9	15.98	9.31E+08	8.64E+08
T235-T150	1.14E+08	2.80E+07	3	6.45	1.52E+08	1.30E+08
	1.14E+08	2.80E+07	6	13.00	6.16E+08	5.21E+08
	1.14E+08	2.80E+07	9	19.64	1.41E+09	1.17E+09

In the tables above, the results of four striking-struck ship combinations are presented. Penetration depth and deformation energy are evaluated with two abovementioned approaches. Based on the results it is easy to conclude that rise in ship speed and mass increases penetration depth and maximum deformation energy. In addition, as expected, the stiffness affects the results also a little.

It can be seen that Minorsky's method gives similar results to Tabri's time-domain model, especially in cases, where ship masses are similar. Otherwise, during striking ship mass increase, the difference between results increases as Minorsky's method slightly underestimates the hydromechanics forces due to the lack of information about hydrodynamic damping. Therefore, the struck ship appears lighter and the amount of deformation energy becomes smaller.

7.2 Collision in ice

This section presents the results of collision calculations in ice by two different methods: time-domain model (Tabri, 2010) and simplified calculation model developed in Section 5.1. All the calculation results are presented in Appendix 2. In addition, simplified collision model calculation approach can be seen in Appendix 3.

Simulations are done similarly to the open water calculations with three different speeds and with two different stiffness's, but the ice force is included based on eq. (4.5). The ice forces are calculated for 150 *m* long struck ship depending on ice thicknesses as was shown Table 7.1. It is seen the ice load increases about 2.41E+06 *N* per 0.5 *m* ice thickness increase. In the ice load calculations the contact length of struck ship side and ice sheet is estimated to be 135 *m.* Stiffness's for calculations are taken same as previously. However figures in below, indicates results where stiffness *k* is 7.29E+06 *N/m.*

Based on the outcomes, in all four cases the deformation energy increased comparing to the open water result. Deformation energy increase depending on ice thickness for different striking speeds are illustrated in Figure 7.1. The reason for deformation energy increase due to the thicker ice should be clear. The thicker the ice is, the larger is the ice bending strength which restricts the transverse movement of struck ship. Therefore, the impact is heavier and deformation energy higher. However if analysing the results, it reflects the increase is not actually particularly significant, see Figure 7.1. The results show the increase of deformation energy, in case of 3 *m/s*, is in an average 6% per 0.5 *m* ice thickness increase. Thus, the difference of deformation energy in between 0.5 *m* ice thickness and 1.5 *m* is approximately 12%. Additionally, comparing the deformation energy in open water and in 1.5 *m* ice, the difference is approximately 19% in low speed. For higher striking speed, as 9 *m/s*, the difference is 6%. However, the highest difference was obtained in collision case T235-T150, where deformation energy increased 20% in 1.5 m thick ice compared to the open water.

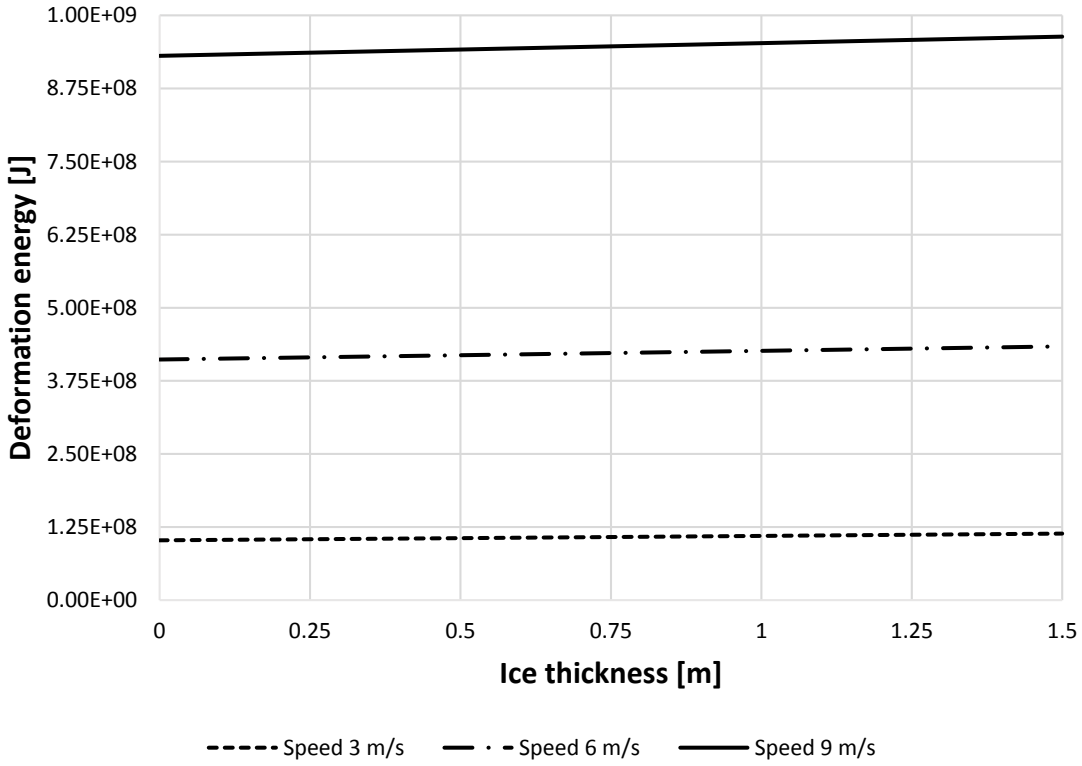

Figure 7.1 Deformation energy in different striking speeds, depending on ice thickness, collision case T190-T150.

Considering penetration depth, then the increase of penetration comparing to the open water is modest, see Figure 7.2. The difference in low speed in open water comparing to 1.5 *m* thick ice is 0.64 *m*. Furthermore, in the last collision scenario penetration depth rises 6.5% when striking velocity is 3 *m/s* and ice thickness increases from 0.5 to 1.5 meters.

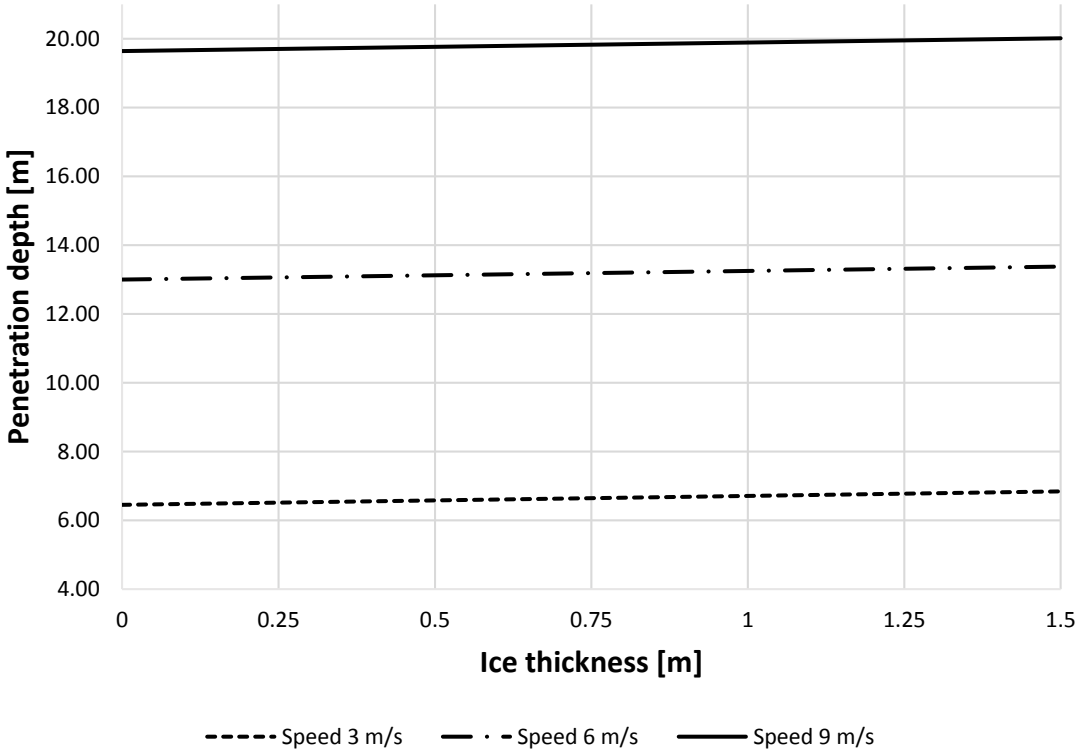

Figure 7.2 Penetration depth in different striking speeds, depending on ice thickness, collision case T235-T150.

In Figure 7.3 is shown the comparison of two calculation approaches. Tabri's model calculates in time-domain and here are presented the maximum values. Looking at the comparison of two different methods in Figure 7.3 a good agreement can be observed. In low speed the difference of deformation energy is 1%, whereas in higher speed the difference is approximately up to 2.2%.

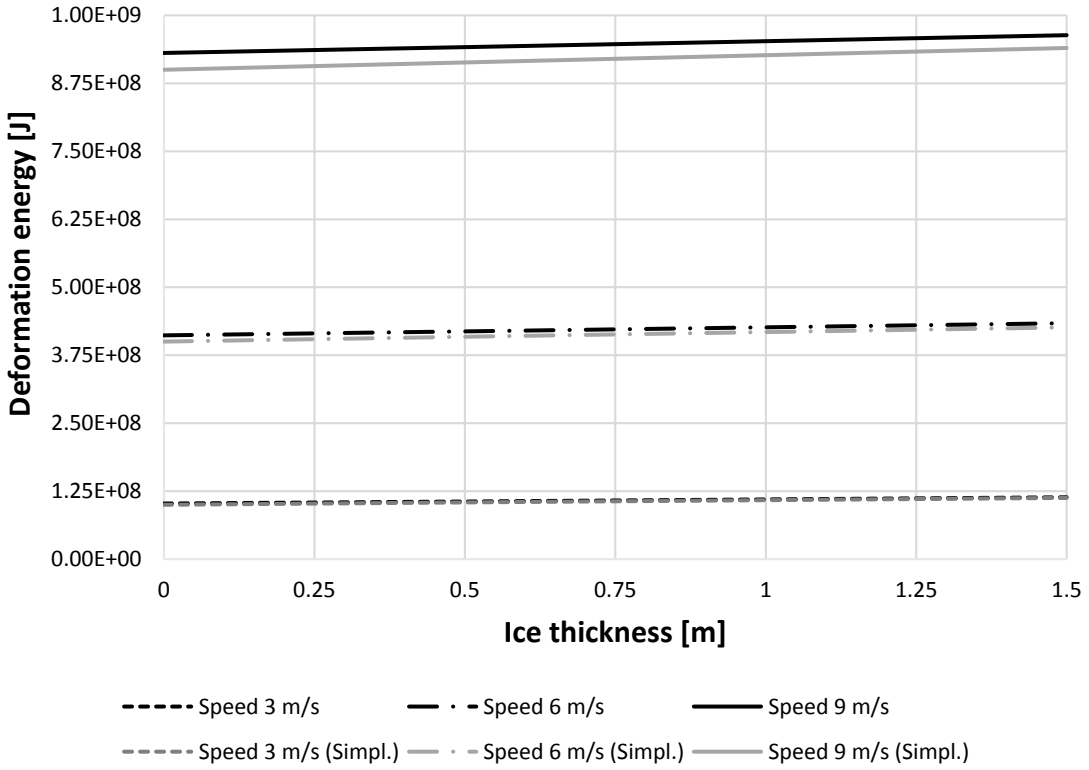

Figure 7.3 Comparison of deformation energy obtained by time-domain model and simplified model, collision case T190-T150.

Comparing the results of penetration depth obtained by two methods, see *Figure 7.4*, the results differ more, especially if following the penetration increase based on striking speeds. The reason for this lies in the matter, that simplified method is not as precise as the time-domain model. As simplified model does not provide the information for the hydrodynamic damping, the model slightly underestimates the hydrodynamic forces. Thus, the struck ship appears lighter and the amount of deformation energy becomes smaller. This effect becomes more important if the duration of the contact increases and the motions of the struck ship become larger. In the case of very short contact duration, the effect of hydrodynamic damping is neglectful. Therefore similarly to deformation energy, in lower speed the agreement is better than in higher speed. Despite of that, still the simplicity of the model is the advantage and the results, which the derived simple model provides, are satisfactory.

In conclusion, it may be stated the simplified model has advantage to estimate results faster than time-domain model. The reason is a simple calculation model comparing to the time-domain model.

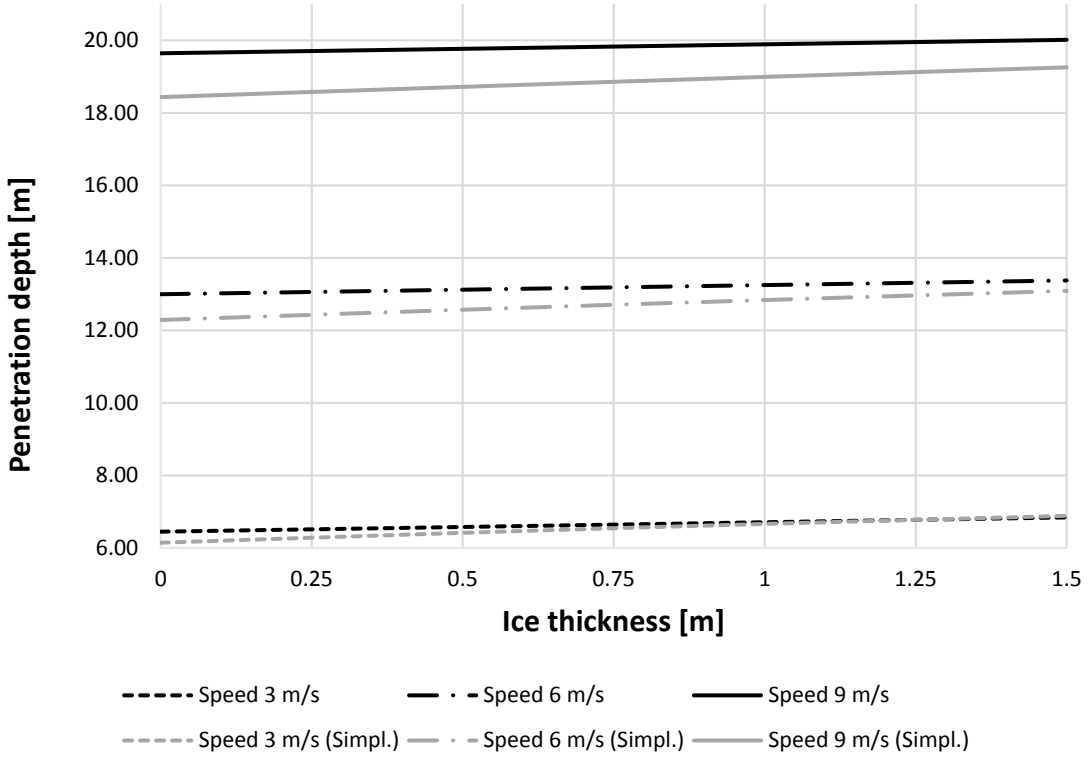

Figure 7.4 Comparison of penetration depth obtained by time-domain model and simplified model, collision case T235-T150.

8 DISCUSSION

As far as the author knows, an analytical ship collision calculation model in ice has not been developed before. Therefore, ice force formula developed for right angle collision scenario is a first attempt to model such collision scenario.

In the present work it was found that the collision calculation in ice does not increase deformation energy and penetration depth significantly compared to the open water collision. The ice force formula developed in the present work was rather simplified. As a result, the ice resistance was relatively low compared to other force components. Therefore, the validity of the ice model in such collision event is still to be studied.

Ice loads were assumed constant during the whole collision event. Although in real conditions, the struck ship movement in low speeds initiates broken ice floes accumulation in front of hull side. This may affect the ice load, as the ice mass increases as a function of time, which in turn, leads to the greater ice forces. Therefore, increase in the ice mass should influence also the deformation energy and the penetration in ship-ship collision, which due to the present approach was not reflected.

In addition, the method used for calculating total horizontal ice force has been developed for sloping structures. Thus during the impact, the ice floes should move underneath the structure. In present work however, the ships that were used in the simulations had quite vertical side structure and there was basically no slope angle. Therefore, the applied Croasdale method may underestimate the ice force for that type of ships. The reason for this lies in the failure process of the ice sheet as the crushing may occur instead of pure bending failure. Thus, the actual ice failure process in case of that kind of ship can be arguable. Another questionable parameter that affects ice force calculation results is the preliminary contact length value l_C. Despite of the slope angle, the value was estimated to be 15 m in all cases. Therefore, this might have affect to the results as well, because contact length l_C was quite sensitive for slope angle in range of 0 to 1 degree.

In the second part of the thesis a simplified collision calculation model in ice showed a good agreement with time-domain model. Although in higher striking speeds the difference increased because simplified model does not consider the hydrodynamic damping which is calculated based on the speed.

In overall it can be stated that the contact length and the slope angle was chosen in a way that it would make calculations easier and simple. Therefore, the assumptions made for calculating the ice force has certainly some affect to the deformation energy and penetration depth results.

9 CONCLUSION AND FUTURE CONSIDERATIONS

The aim of the thesis was to develop simplified ice force formula for a case where ship collides with an ice in transverse direction. Necessity for the formula is justified due to the rapid increase of marine traffic in the Northern Baltic Sea where the ice can remain up to several months. Therefore, the possibility having collision in severe and changing ice conditions is relatively high.

The ice force method in this thesis was developed and validated on the basis of the line load curves obtained from SAFEWIN model tests (Filipović, 2014) and based on line load curve from ice damage statistics report (Kujala, 1991). The ice force, which includes also Croasdale's 2-D horizontal ice force calculation method, showed satisfactory results comparing to the line loads measured in SAFEWIN model testing. In addition, the ice conditions in the Baltic Sea was studied to characterize the winter navigation conditions.

The developed ice force formula was added to the collision calculations where ship collides with another at a 90 degrees angle in ice. The ship collision in ice was calculated with time-domain model (Tabri, 2010), while the open water collision was calculated with a model based on the conservation of momentum (Minorsky, 1959). As the time-domain approach is rather complicated, a simplified calculation model based on the conservation of momentum including the ice force was derived.

The results of the collision calculations where the ice was included to the simulations did not significantly increase the deformation energy and penetration depth of struck ship comparing to the open water collision. Deformation energy increases approximately up to 20% compared to the open water. In calculations most of the energy was absorbed before the ships reached to common velocity and the energy absorbed by ice was relatively small compared to other energy absorbing mechanisms. This reveals the ice force calculated with present approach is small compared to other force components, such as collision force and inertia force. The reason for this may lie in the fact that the ice force formula slightly underestimates the actual force, because

ice force is developed as constant value. Although in real situation, the ice cusps starts to accumulate in front of the hull side, which in turn increases ice mass in time. Therefore, ice force should increase as well.

Nevertheless, derived simplified calculation model for collision in ice showed good agreement with the results obtained by time-domain model. Therefore, applying simplified model for calculations is easier and helps to reach to the result faster.

However in future studies, due to the lack of information about collision in ice, there is a need for model testing to obtain experimental validation data. In addition, as the Croasdale's ice force model is based on the sloping structures the ice force should be calculated also for a ship which has larger slope angle than 1 degrees, for example for 10 degrees. Therefore, it could be seen how well the ice force results agree to experimental data. Furthermore, in the present method certain variables are applied and all the results are based on point estimates. However in future studies could adopt certain distributions for the variables to see how results would vary. Finally, the method could also consider the ice accumulation in front of the hull during the impact to simulate conditions more similar to real situation.

KOKKUVÕTE

Meretranspordi süsteem Läänemere põhjaosas on keeruline ja toimib vägagi erinevates keskkonnatingimustes. Kõige keerulisemad tingimused tulenevad jääoludest, mis Soome lahes või Botnia lahes võivad püsida kuni mitu kuud. Seetõttu on ilmne, et õnnetuste arv nendes kahes regioonis on kõrgeim talvehooajal, mis võib hõlmata õnnetusi nagu laeva karile sõit, laevade vahelised kokkupõrked ja muid jääst tulenevaid kahjustusi

Antud töös otsitakse lihtsustatud meetodit hindamaks jääst tulenevat koormust juhul, kui laev põrkab jääga kokku ristisuunas liikudes. Tuletatud jääkoormuse valem lisatakse dünaamilisele kokkupõrke mudelile hindamaks kokkupõrke kahjustusi. Lisaks on tuletatud edasi Minorsky klassikalist kokkupõrke mudelit, arvestamaks jääst tulenevat mõju.

Jääkoormuse arvutusmudel töötati välja põhinedes jää jõu arvutamise mudelile laiadele kaldpinnaga avamere ehitistele ja samuti SAFEWIN projekti raames saadud mudelkatsete tulemustele. Mudel valideeriti jää kahjustuste statistika aruande põhjal. Kokkupõrke arvutused jääs tehti aegruumis opereeriva mudeliga ning võrreldi lihtsustatud mudeliga.

Tuletatud jääkoormuse valem näitas rahuldavat vastavust võrreldes SAFEWIN mudelkatsete tulemustega. Samuti näitas lihtsustatud kokkupõrke arvutusmudel head kooskõla aegruumis opereeriva mudeliga. Võrreldes avavees saadud tulemustega seisnes peamine erinevus laeva virtuaalses massi kasvamises jää tõttu. Seetõttu deformatsioonienergia ja sissetungisügavus suurenes. Deformatsiooni energia suurenemine võrreldes avavees saadud tulemustega ei olnud märkimisväärne, kuna antud lähenemisviisil arvutatud jää jõu komponendi mõju on väike võrreldes kontakt- ja inertsijõuga.

SUMMARY

The maritime transportation system in the Northern Baltic Sea (NBS) is complex and operates under varying environmental conditions. The most challenging conditions relate to the presence of ice-cover, which for the NBS i.e. Gulf of Finland or Bay of Bothnia, can remain up to several months. Therefore it is evident, that the number of accidents in these two areas is the highest during winter season which can involve accidents like groundings, collisions and damages due to the ice.

This thesis seeks for a simplified method for evaluating the ice force for a case where ship collides with ice in transverse direction. The derived ice force formula is added to the time-domain collision simulation model for the evaluation of collision damage. Additionally, Minorsky's classical collision model is developed further to consider the influence of ice in ship collision dynamics.

The ice force calculation model was developed based on the knowledge of calculating ice force for wide sloping offshore structures and based on the model test results measured during SAFEWIN project. The model was validated on the basis of ice damage statistics report. The collision calculations in ice were done by time-domain model and compared to the developed simple model.

As a result, the ice force formula showed satisfactory agreement compared to the SAFEWIN project model test results. Derived simplified collision calculation model revealed a good agreement with time-domain model. In comparison with open water results, the main change in collision in ice came from the added mass increase due to the ice. Therefore, deformation energy and penetration depth rose. In calculations, the increase in deformation energy, compared to the open water result was however not significant as the ice forces evaluated with the present model are small compared to other forces such as collision and inertia force.

BIBLIOGRAPHY

Chen, D., 2000. *Simplified ship collision model.* Virginia: Virginia Polytechnic Institute and State University.

Croasdale, K., 1980. *Ice forces on fixed, rigid structures.,* USA: s.n.

Filipović, A., 2014. *Evaluation of ice induced loads on ships in compressive ice.* Zagreb: University of Zagreb.

Granskog, M. et al., 2006. Sea ice in the Baltic Sea e A review. *Estuarine, Coastal and Shelf Science,* pp. 145-160.

Hänninen, S., 2003. *Ship Based Observations on Board MT Uikku during the Winter 2003.,* s.l.: s.n.

ISO 19906, 2010. *Petroleum and natural gas industries - Arctic Offshore Structures 2010-15-12.* First ed. Switzerland: s.n.

Kotisalo, K. & Kujala, P., 1999. *Ice load measurements onboard MT Uikku during the ARCDEV voyage.* s.l., s.n., pp. 974-987.

Kujala, P., 1991. *Damage statistics of ice-strengthened ships in the Baltic Sea 1984-1987. Report. No. 50.,* Espoo: Winter Navigation Research Board.

Kujala, P., 1994. *On the statistics of ice loads on ship hull in the Baltic.* Helsinki: Acta Polutechnica Scandinavica, Mechanical Engineering Series No. 116.

Kujala, P. & Arughadhoss, S., 2012. Statistical Analysis of Ice Crushing Pressures on a Ship's Hull During Hull-Ice Interaction. *Cold Regions Science and Technology, no. 70,* pp. 1-11.

Kujala, P. & Riska, K., 2010. *Talvimerenkulku (TKK-AM-13-2010).* Espoo: Helsinki University of Technology.

Kujala, P., Valkonen, J. & Suominen, M., 2007. *Maximum ice induced loads on ships in the Baltic Sea.* Houston October 1-5, 2007, s.n.

Külaots, R., 2012. *Numerical and experimental modelling of ship resistance in compressive ice channels.* Espoo: Aalto University.

Leppäranta, M. & Myrberg, K., 2009. The ice of the Baltic Sea. In: *Physical Oceanography of the Baltic Sea.* s.l.:Springer Berlin Heidelberg, pp. 219-260.

Lindqvist, G., 1989. *Straightforward Method for Calculation of Ice Resistance of Ships.* s.l., s.n., pp. p722-735.

Liu, Z., 2011. *Analytical and numerical analysis of iceberg collisions with ship structures.* Trondheim: Norweigan University of Science and Technology.

Lubbad, R. & Løset, S., 2011. A numerical model for real-time simulation of ship–ice interaction. 65(2), pp. 111-127.

Minorsky, V., 1959. An analysis of ship collision with reference to protection of nuclear power plants. *Journal of Ship Research,* Volume 3, pp. 1-4.

Petersen, M. J., 1982. Dynamics of Ship Collision. 9(4), pp. 295-329.

Riska, K., 2011. *Ship – ice interaction in ship design: theory and practice.* s.l.:NTNU.

Riska, K., Wilhelmson, M., Englund, K. & Leiviskä, T., 1997. *Performance of Merchant Vessels in Ice in the Baltic. Research Report No 52,* Espoo: Winter Navigation Research Board.

Seinä, A., 2008. *The Baltic Sea portal.* [Online]
Available at:
http://www.itameriportaali.fi/en/ajankohtaista/mtl_uutisarkisto/2008/en_GB/polar_view
[Accessed 15 April 2014].

Su, B., 2011. *Numerical predictions of global and local ice loads on ships.* Trondheim: Norweigan University of Science and Technology.

Suominen, M. & Montewka, J., 2012. *Model Testing Results WP4 for SAFEWIN,* Espoo: Aalto University (internal report).

Tabri, K., 2010. *Dynamics of Ship Collision.* Espoo: Aalto University.

The Baltic Sea portal, 2014. [Online]
Available at: http://www.itameriportaali.fi/en/tietoa/jaa/en_GB/millaista_jaata_esiintyy/
[Accessed 15 April 2014].

Tomac, T. et al., 2013. *Numerical simulations of ship resistance in model ice.* s.l., s.n., pp. 847-851.

Valkonen, J., Cammaert, G. & Mejlænder-Larsen, M., 2008. *Field program for simulation of station-keeping conditions for Arctic drilling and production vessels.*. Banff, Canada, s.n.

Vihma, T. & Haapala, J., 2009. Geophysics of sea ice in the Baltic Sea: A review. *Progress in Oceanography,* September, 82(3-4), pp. 129-148.

von Bock und Polach, R. & Ehlers, S., 2013. Model scale ice — Part B: Numerical model. Volume 94, pp. 53-60.

Zhang, S., 1999. *The mechanics of ship collisions.* s.l.:Technical University of Denmark.

Zhou, L., Riska, K., Moan, T. & Su, B., 2012. Numerical modelling of ice loads on an icebreaker tanker: Comparing simulations with model tests. *Cold Regions Science and Technology,* Volume 87.

Zhou, L. et al., 2012. Experiments on level ice loading on an icebreaking tanker with different ice drift angles. *Cold regions Science and Technology,* Volume 85.

APPENDIX 1

Line load calculation for Credo model.

1. Line load calculation if slope angle is α=1deg, ice thickness is 40 mm.

Flexural strength $\sigma_f := 30.8 \cdot 10^3$ Pa

Elastic modulus $E_i := 51 \cdot 10^6$ Pa

Density of water $\rho_w := 1004$ $\frac{kg}{m^3}$

Density of ice $\rho_i := 900$ $\frac{kg}{m^3}$

Ice thickness $h_i := 0.04$ m

Ice-hull friction $\mu := 0.09$

Acceleration of gravity $g := 9.81$ $\frac{m}{s^2}$

Slope angle $\alpha := 1deg$

Density difference $\delta\rho := (\rho_w - \rho_i)$

Breaking load component

$$\xi := \frac{\sin(\alpha) + \mu \cdot \cos(\alpha)}{\cos(\alpha) - \mu \cdot \sin(\alpha)} = 0.108$$

$$H_B := 0.68 \cdot \xi \cdot \sigma_f \cdot \left(\frac{\rho_w \cdot g \cdot h_i^5}{E_i} \right)^{0.25} = 4.753 \quad \frac{N}{m}$$

Ride-down force component

Height from waterline to the bottom of stucture(Draft)

$z := 0.35$ m

$$H_R := z \cdot h_i \cdot \delta\rho \cdot g \cdot (\sin(\alpha) + \mu \cdot \cos(\alpha)) \cdot \left(\frac{\sin(\alpha) + \mu \cdot \cos(\alpha)}{\cos(\alpha) - \mu \cdot \sin(\alpha)} + \frac{\cos(\alpha)}{\sin(\alpha)} \right) = 88.082 \quad \frac{N}{m}$$

Horizontal ice force

$$q_{Croasdale} := H_B + H_R = 92.835 \quad \frac{N}{m}$$

Parameter C value for line load

$l_c := 15$ m Estimated contact length (Based on A.Filipović thesis)

$s := 0.014$ m frame spacing in model scale

Deriving C value from line load equation:

$$C_1 := \frac{q_{Croasdale}}{\left(\frac{l_c}{s} \right)^{-0.71}} = 1.315 \times 10^4 \quad \frac{N}{m}$$

$q_{C1}(L) := 9182.4 \cdot \left(\frac{L}{s} \right)^{-0.546}$ Fitted line load curve (Filipović, 2014).

$q_1(L) := C_1 \cdot \left(\frac{L}{s} \right)^{-0.71} \cdot 2.6$ Line load obtained based on present work method

$L := 0, 0.01 .. 150$

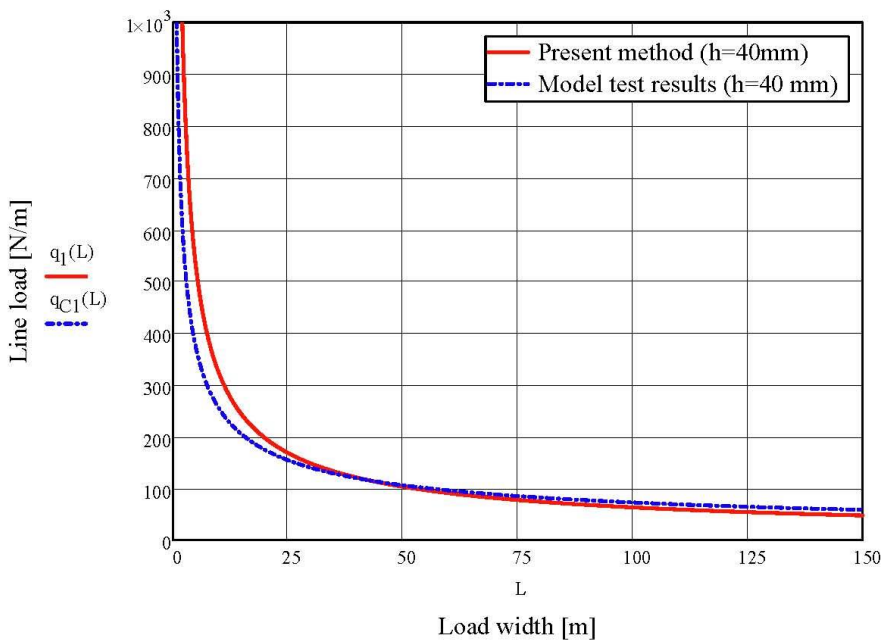

Ice thickness is 29 mm

Flexural strength	$\sigma_f := 29.5 \cdot 10^3$	Pa
Elastic modulus	$E_i := 65.3 \cdot 10^6$	Pa
Ice thickness	$h_i := 0.029$	m

Breaking load component

$$\xi := \frac{\sin(\alpha) + \mu \cdot \cos(\alpha)}{\cos(\alpha) - \mu \cdot \sin(\alpha)} = 0.108$$

$$H_B := 0.68 \cdot \xi \cdot \sigma_f \cdot \left(\frac{\rho_w \cdot g \cdot h_i^5}{E_i} \right)^{0.25} = 2.863 \quad \frac{N}{m}$$

Ride-down force component

Height from waterline to the bottom of stucture (Draft)

$z := 0.35 \ m$

$$H_D := z \cdot h_i \cdot \delta\rho \cdot g \cdot (\sin(\alpha) + \mu \cdot \cos(\alpha)) \cdot \left(\frac{\sin(\alpha) + \mu \cdot \cos(\alpha)}{\cos(\alpha) - \mu \cdot \sin(\alpha)} + \frac{\cos(\alpha)}{\sin(\alpha)} \right) = 63.859 \quad \frac{N}{m}$$

Horizontal ice force

$q_{Croasdale} := H_B + H_R = 66.722 \ \frac{N}{m}$

Parameter C value for line load

$l_c := 15 \ m$ Estimated contact length (Based on A.Filipović thesis)

$s := 0.014 \ m$ frame spacing in model scale

Deriving C value from line load equation:

$$C_5 := \frac{q_{Croasdale}}{\left(\frac{l_c}{s}\right)^{-0.71}} = 9.452 \times 10^3 \ \frac{N}{m}$$

$q_{C5}(L) := 3054.6 \cdot \left(\frac{L}{s}\right)^{-0.427}$ Fitted line load curve (Filipović, 2014).

$q_5(L) := C_5 \cdot \left(\frac{L}{s}\right)^{-0.71}$ 2.6 Line load obtained based on present work method

$L := 0, 0.01 .. 150$

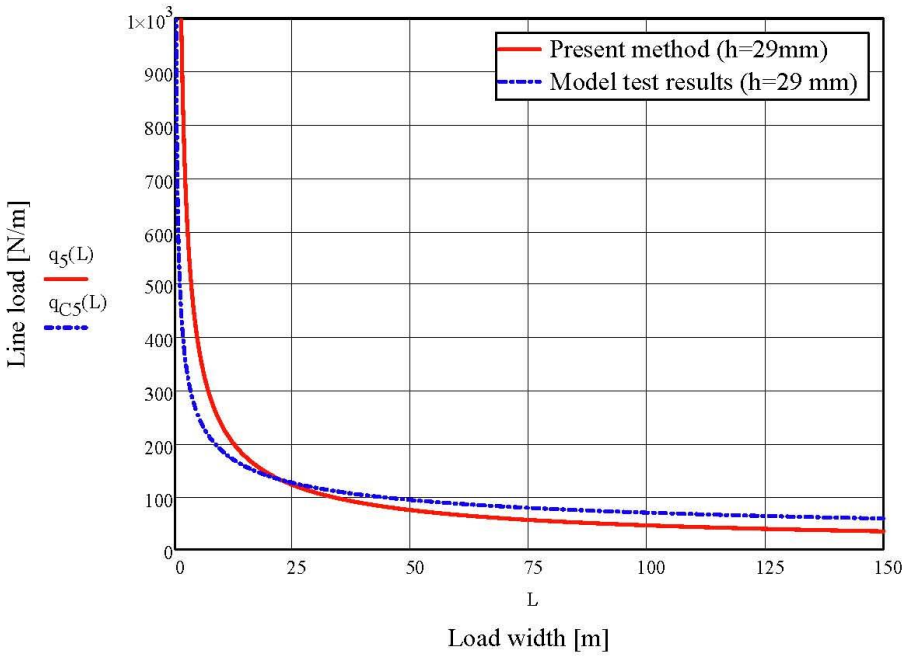

Ice thickness is 24 mm

Flexural strength $\sigma_f := 22.9 \cdot 10^3$ Pa

Elastic modulus $E_i := 63.15 \cdot 10^6$ Pa

Ice thickness $h_i := 0.024$ m

Breaking load component

$$\xi := \frac{\sin(\alpha) + \mu \cdot \cos(\alpha)}{\cos(\alpha) - \mu \cdot \sin(\alpha)} = 0.108$$

$$H_B := 0.68 \cdot \xi \cdot \sigma_f \cdot \left(\frac{\rho_w \cdot g \cdot h_i^5}{E_i} \right)^{0.25} = 1.769 \quad \frac{N}{m}$$

Ride-down force component

Height from waterline to the bottom of stucture (Draft)

$z := 0.35$ m

$$H_R := z \cdot h_i \cdot \delta\rho \cdot g \cdot (\sin(\alpha) + \mu \cdot \cos(\alpha)) \cdot \left(\frac{\sin(\alpha) + \mu \cdot \cos(\alpha)}{\cos(\alpha) - \mu \cdot \sin(\alpha)} + \frac{\cos(\alpha)}{\sin(\alpha)} \right) = 52.849 \quad \frac{N}{m}$$

Horizontal ice force

$$q_{Croasdale} := H_B + H_R = 54.618 \quad \frac{N}{m}$$

Parameter C value for line load

$l_c := 15$ m Estimated contact length (Based on A.Filipović thesis)

$s := 0.014$ m Frame spacing in model scale

Deriving C value from line load equation:

$$C_6 := \frac{q_{Croasdale}}{\left(\frac{l_c}{s} \right)^{-0.71}} = 7.738 \times 10^3 \quad \frac{N}{m}$$

$q_{C6}(L) := 2983.1 \cdot \left(\frac{L}{s} \right)^{-0.5}$ Fitted line load curve (Filipović, 2014).

$q_6(L) := C_6 \cdot \left(\frac{L}{s} \right)^{-0.71}$ 2.6 Line load obtained based on present work method

$L := 0, 0.01 .. 150$

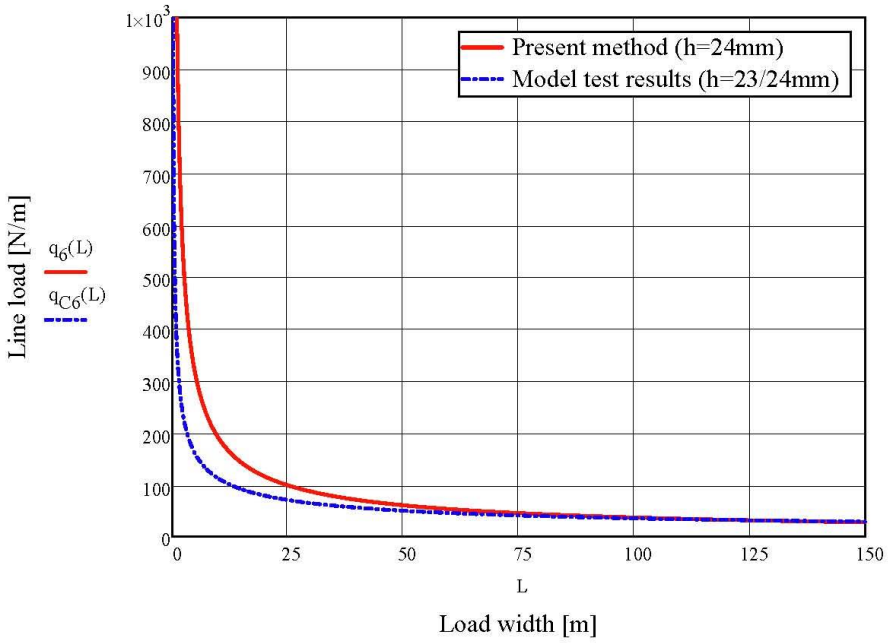

Comparison of line loads with Kujala(1991) report, ice thickness 70 cm

Input data

Flexural strength	$\sigma_f := 580 \cdot 10^3$	Pa
Elastic modulus	$E := 5 \cdot 10^9$	Pa
Density of water	$\rho_w := 1004$	$\frac{kg}{m^3}$
Density of ice	$\rho_i := 900$	$\frac{kg}{m^3}$
Ice thickness	$h_i := 0.7$	m
Ice-hull friction	$\mu := 0.1$	
Acceleration of gravity	$g := 9.81$	$\frac{m}{s^2}$
Slope angle	$\alpha := 1deg$	
Density difference	$\delta\rho := (\rho_w - \rho_i)$	
Draft	$T := 9.2$	m

Breaking load component

$$\xi := \frac{\sin(\alpha) + \mu \cdot \cos(\alpha)}{\cos(\alpha) - \mu \cdot \sin(\alpha)} = 0.118$$

$$H_B := 0.68 \cdot \xi \cdot \sigma_f \cdot \left(\frac{\rho_w \cdot g \cdot h_i^{\,5}}{E_i} \right)^{0.25} = 1.113 \times 10^{6} \frac{N}{m}$$

Ride-down force component

Height from waterline to the bottom of stucture(Draft)

$z := T = 9.2 \quad m$

$$H_R := z \cdot h_i \cdot \delta\rho \cdot g \cdot (\sin(\alpha) + \mu \cdot \cos(\alpha)) \cdot \left(\frac{\sin(\alpha) + \mu \cdot \cos(\alpha)}{\cos(\alpha) - \mu \cdot \sin(\alpha)} + \frac{\cos(\alpha)}{\sin(\alpha)} \right) = 4.43 \times 10^{4} \quad \frac{N}{m}$$

Horizontal ice force

$$q_{Croasdale} := H_B + H_R = 4.541 \times 10^{4} \quad \frac{N}{m}$$

Parameter C value for line load

$l_c := 15 \quad m$

$s := 0.35 \quad m$ frame spacing

Deriving C value from line load equation:

$$C_{1v} := \frac{q_{Croasdale}}{\left(\frac{l_c}{s}\right)^{-0.71}} = 6.545 \times 10^{5} \quad \frac{N}{m} \qquad C_{ice\_old} := \frac{q_{Croasdale}}{\left(\frac{l_c}{s}\right)^{-0.71}} = 6.545 \times 10^{5} \quad \frac{N}{m}$$

Ice load from line load

Coefficient for line load fitting

$$q_{ice\_old}(L) := C_{ice\_old} \cdot \left(\frac{L}{s}\right)^{-0.71} \qquad C_1 \cdot \left(\frac{1}{s}\right)^{-0.71} = 3.106 \times 10^{5} \qquad k := \frac{814}{310} = 2.626$$

$$q_{ice\_new}(L) := C_1 \cdot \left(\frac{L}{s}\right)^{-0.71} \cdot 2.6$$ Line load multiplied with coefficient

Line load eq. from Kujala report:

$$q_{kujala}(L) := \left(814 L^{-0.71}\right) 1000$$

L := 0, 0.001 .. 150

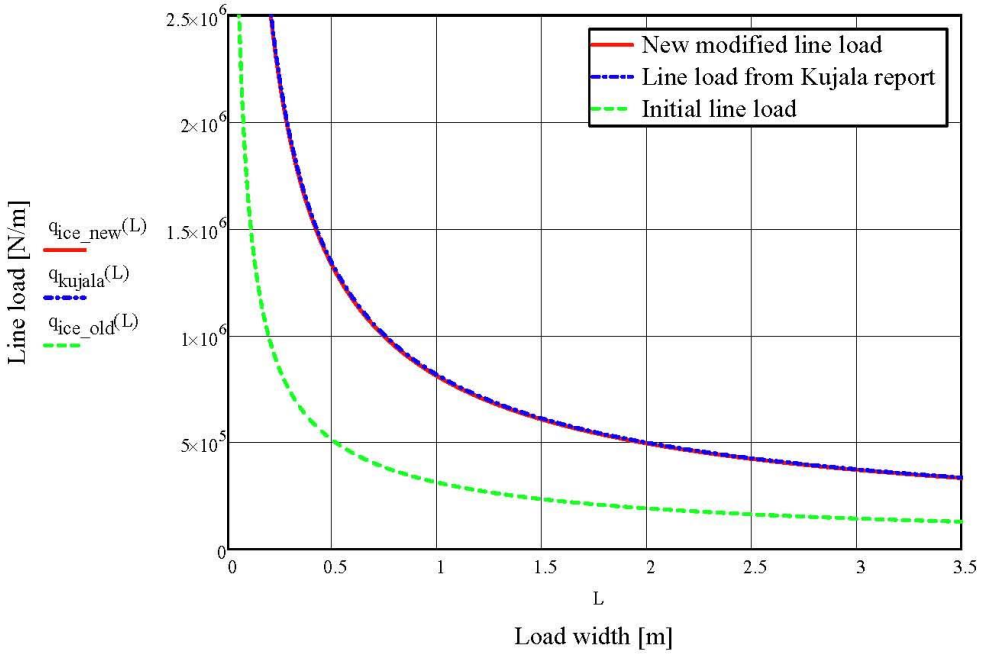
New modified line load
Line load from Kujala report
Initial line load
Line load [N/m]
$q_{ice\_new}(L)$
$q_{kujala}(L)$
$q_{ice\_old}(L)$
2.5×10^6
2×10^6
1.5×10^6
1×10^6
5×10^5
0
0
0.5
1
1.5
2
2.5
3
3.5
L
Load width [m]

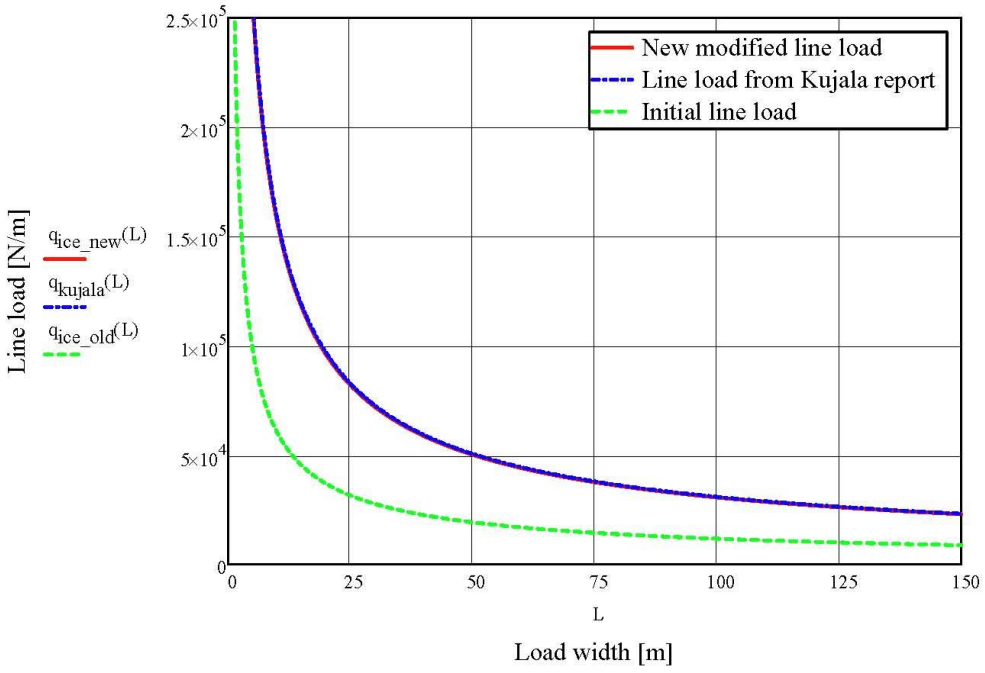
New modified line load
Line load from Kujala report
Initial line load
Line load [N/m]
$q_{ice\_new}(L)$
$q_{kujala}(L)$
$q_{ice\_old}(L)$
2.5×10^5
2×10^5
1.5×10^5
1×10^5
5×10^4
0
0
25
50
75
100
125
150
L
Load width [m]

APPENDIX 2

Table A2.1 Result of collision in ice when k is 1.46E+07 N/m.

Collision scenario (Striking-Struck ship)	Striking velocity V_A[m/s]	Def. energy with Minorsky's model (no ice) [J]	Ice thickness h_i [m]	Ice load [N]	Def. energy with time-domain model [J]	Def. energy with simple model [J]
T120-T150	3	4.51E+07	0	0	4.52E+07	4.59E+07
	6	1.80E+08	0		1.81E+08	1.84E+08
	9	4.06E+08	0		4.07E+08	4.13E+08
	3	4.51E+07	0.5	2.39E+06	4.67E+07	4.69E+07
	6	1.80E+08	0.5		1.84E+08	1.86E+08
	9	4.06E+08	0.5		4.11E+08	4.16E+08
	3	4.51E+07	1	4.80E+06	4.82E+07	4.79E+07
	6	1.80E+08	1		1.87E+08	1.88E+08
	9	4.06E+08	1		4.16E+08	4.19E+08
	3	4.51E+07	1.5	7.21E+06	4.98E+07	4.88E+07
	6	1.80E+08	1.5		1.90E+08	1.90E+08
	9	4.06E+08	1.5		4.20E+08	4.22E+08
T150-T150	3	7.46E+07	0	0	7.44E+07	7.71E+07
	6	2.99E+08	0		2.98E+08	3.08E+08
	9	6.72E+08	0		6.71E+08	6.93E+08
	3	7.46E+07	0.5	2.39E+06	7.75E+07	7.98E+07
	6	2.99E+08	0.5		3.04E+08	3.14E+08
	9	6.72E+08	0.5		6.80E+08	7.02E+08
	3	7.46E+07	1	4.80E+06	8.07E+07	8.24E+07
	6	2.99E+08	1		3.10E+08	3.19E+08
	9	6.72E+08	1		6.90E+08	7.10E+08
	3	7.46E+07	1.5	7.21E+06	8.41E+07	8.50E+07
	6	2.99E+08	1.5		3.17E+08	3.25E+08
	9	6.72E+08	1.5		6.99E+08	7.18E+08
T190-T150	3	9.60E+07	0	0	9.95E+07	1.00E+08
	6	3.84E+08	0		3.99E+08	4.00E+08
	9	8.64E+08	0		9.02E+08	9.00E+08

	3	9.60E+07	0.5	2.39E+06	1.04E+08	1.05E+08
	6	3.84E+08	0.5		4.08E+08	4.10E+08
	9	8.64E+08	0.5		9.15E+08	9.15E+08
	3	9.60E+07	1	4.80E+06	1.09E+08	1.10E+08
	6	3.84E+08	1		4.18E+08	4.20E+08
	9	8.64E+08	1		9.29E+08	9.19E+08
	3	9.60E+07	1.5	7.21E+06	1.14E+08	1.09E+08
	6	3.84E+08	1.5		4.27E+08	4.19E+08
	9	8.64E+08	1.5		9.43E+08	9.31E+08
T235-T150	3	1.30E+08	0	0	1.41E+08	1.38E+08
	6	5.21E+08	0		5.69E+08	5.51E+08
	9	1.17E+09	0		1.29E+09	1.24E+09
	3	1.30E+08	0.5	2.39E+06	1.48E+08	1.52E+08
	6	5.21E+08	0.5		5.84E+08	5.80E+08
	9	1.17E+09	0.5		1.31E+09	1.28E+09
	3	1.30E+08	1	4.80E+06	1.56E+08	1.65E+08
	6	5.21E+08	1		5.99E+08	6.08E+08
	9	1.17E+09	1		1.34E+09	1.33E+09
	3	1.30E+08	1.5	7.21E+06	1.65E+08	1.78E+08
	6	5.21E+08	1.5		6.15E+08	6.36E+08
	9	1.17E+09	1.5		1.36E+09	1.37E+09

Table A2.2 Result of collision in ice when k is 7.29E+06 N/m.

Striking-Struck ship	**Striking velocity V_A[m/s]**	**Def. energy with Minorsky's model (no ice) [J]**	**Ice thickness h_i [m]**	**Ice load [N]**	**Def. energy with time-domain model [J]**	**Def. energy with simple model [J]**
T120-T150	3	4.51E+07	0	0	4.50E+07	4.59E+07
	6	1.80E+08	0		1.80E+08	1.84E+08
	9	4.06E+08	0		4.05E+08	4.13E+08
	3	4.51E+07	0.5	2.39E+06	4.70E+07	4.73E+07
	6	1.80E+08	0.5		1.84E+08	1.87E+08
	9	4.06E+08	0.5		4.11E+08	4.18E+08
	3	4.51E+07	1	4.80E+06	4.91E+07	4.87E+07
	6	1.80E+08	1		1.88E+08	1.89E+08
	9	4.06E+08	1		4.17E+08	4.22E+08
	3	4.51E+07	1.5	7.21E+06	5.13E+07	5.00E+07
	6	1.80E+08	1.5		1.92E+08	1.92E+08
	9	4.06E+08	1.5		4.23E+08	4.26E+08

T150-T150	3	7.46E+07	0	0	7.40E+07	7.71E+07
	6	2.99E+08	0		2.97E+08	3.08E+08
	9	6.72E+08	0		6.69E+08	6.93E+08
	3	7.46E+07	0.5	2.39E+06	7.80E+07	8.09E+07
	6	2.99E+08	0.5		3.04E+08	3.16E+08
	9	6.72E+08	0.5		6.80E+08	7.05E+08
	3	7.46E+07	1	4.80E+06	8.23E+07	8.46E+07
	6	2.99E+08	1		3.13E+08	3.24E+08
	9	6.72E+08	1		6.92E+08	7.17E+08
	3	7.46E+07	1.5	7.21E+06	8.67E+07	8.81E+07
	6	2.99E+08	1.5		3.21E+08	3.31E+08
	9	6.72E+08	1.5		7.04E+08	7.28E+08
T190-T150	3	9.60E+07	0	0	1.02E+08	1.00E+08
	6	3.84E+08	0		4.12E+08	4.00E+08
	9	8.64E+08	0		9.31E+08	9.00E+08
	3	9.60E+07	0.5	2.39E+06	1.09E+08	1.07E+08
	6	3.84E+08	0.5		4.24E+08	4.14E+08
	9	8.64E+08	0.5		9.48E+08	9.22E+08
	3	9.60E+07	1	4.80E+06	1.15E+08	1.14E+08
	6	3.84E+08	1		4.36E+08	4.29E+08
	9	8.64E+08	1		9.66E+08	9.43E+08
	3	9.60E+07	1.5	7.21E+06	1.22E+08	1.20E+08
	6	3.84E+08	1.5		4.49E+08	4.42E+08
	9	8.64E+08	1.5		9.85E+08	9.64E+08
T235-T150	3	1.30E+08	0	0	1.52E+08	1.38E+08
	6	5.21E+08	0		6.16E+08	5.51E+08
	9	1.17E+09	0		1.41E+09	1.24E+09
	3	1.30E+08	0.5	2.39E+06	1.62E+08	1.58E+08
	6	5.21E+08	0.5		6.36E+08	5.92E+08
	9	1.17E+09	0.5		1.44E+09	1.30E+09
	3	1.30E+08	1	4.80E+06	1.72E+08	1.76E+08
	6	5.21E+08	1		6.56E+08	6.31E+08
	9	1.17E+09	1		1.47E+09	1.36E+09
	3	1.30E+08	1.5	7.21E+06	1.83E+08	1.92E+08
	6	5.21E+08	1.5		6.77E+08	6.68E+08
	9	1.17E+09	1.5		1.50E+09	1.42E+09

Table A2.3 Comparison of penetration depth in collision in ice when k is 1.46E+07 N/m.

Striking-Struck ship	Striking velocity V_A [m/s]	Ice thickness h_i [m]	Transverse penetration with time-domain model [m]	Penetration increase of time-domain model [%]	Transverse penetration with simplified model [m]	Penetration increase of simplified model [%]
T120-T150	3	0	2.49	0.00%	2.51	0.00%
	6	0	4.98	0.00%	5.02	0.00%
	9	0	7.47	0.00%	7.53	0.00%
	3	0.5	2.53	1.65%	2.54	1.08%
	6	0.5	5.02	0.82%	5.05	0.54%
	9	0.5	7.51	0.54%	7.56	0.36%
	3	1	2.57	3.33%	2.56	2.11%
	6	1	5.06	1.65%	5.07	1.06%
	9	1	7.55	1.09%	7.58	0.72%
	3	1.5	2.61	5.05%	2.59	3.11%
	6	1.5	5.10	2.49%	5.10	1.59%
	9	1.5	7.59	1.65%	7.61	1.06%
T150-T150	3	0	3.19	0.00%	3.25	0.00%
	6	0	6.39	0.00%	6.50	0.00%
	9	0	9.60	0.00%	9.75	0.00%
	3	0.5	3.26	2.06%	3.31	1.81%
	6	0.5	6.46	1.02%	6.56	0.89%
	9	0.5	9.66	0.67%	9.81	0.59%
	3	1	3.33	4.17%	3.36	3.41%
	6	1	6.52	2.05%	6.62	1.77%
	9	1	9.73	1.36%	9.87	1.18%
	3	1.5	3.40	6.32%	3.42	5.04%
	6	1.5	6.59	3.10%	6.67	2.61%
	9	1.5	9.79	2.05%	9.92	1.76%
T190-T150	3	0	3.69	0.00%	3.70	0.00%
	6	0	7.40	0.00%	7.41	0.00%
	9	0	11.12	0.00%	11.11	0.00%
	3	0.5	3.78	2.31%	3.80	2.59%
	6	0.5	7.48	1.14%	7.50	1.28%

	9	0.5	11.20	0.75%	11.21	0.86%
	3	1	3.87	4.67%	3.88	4.95%
	6	1	7.57	2.29%	7.59	2.52%
	9	1	11.29	1.51%	11.23	1.04%
	3	1.5	3.95	7.08%	3.87	4.57%
	6	1.5	7.66	3.46%	7.58	2.32%
	9	1.5	11.37	2.28%	11.30	1.69%
T235-T150	3	0	4.40	0.00%	4.35	0.00%
	6	0	8.83	0.00%	8.69	0.00%
	9	0	13.31	0.00%	13.04	0.00%
	3	0.5	4.51	2.64%	4.57	5.09%
	6	0.5	8.95	1.30%	8.92	2.64%
	9	0.5	13.43	0.86%	13.27	1.78%
	3	1	4.63	5.35%	4.76	9.60%
	6	1	9.06	2.62%	9.13	5.11%
	9	1	13.54	1.72%	13.49	3.49%
	3	1.5	4.75	8.10%	4.94	13.65%
	6	1.5	9.18	3.95%	9.34	7.43%
	9	1.5	13.66	2.59%	13.703	5.12%

Table A2.4 Comparison of penetration depth in collision in ice when k is 7.29E+06 N/m.

Striking-Struck ship	Striking velocity V_A [m/s]	Ice thickness h_i [m]	Transverse penetration with time-domain model [m]	Penetration increase of time-domain model [%]	Transverse penetration with simplified model [m]	Penetration increase of simplified model [%]
T120-T150	3	0	3.51	0.00%	3.55	0.00%
	6	0	7.03	0.00%	7.10	0.00%
	9	0	10.54	0.00%	10.65	0.00%
	3	0.5	3.59	2.21%	3.60	1.46%
	6	0.5	7.11	1.09%	7.15	0.76%
	9	0.5	10.62	0.72%	10.70	0.50%
	3	1	3.67	4.47%	3.65	2.93%
	6	1	7.18	2.21%	7.21	1.49%
	9	1	10.70	1.46%	10.76	1.00%
	3	1.5	3.75	6.78%	3.70	4.31%
	6	1.5	7.26	3.33%	7.26	2.23%
	9	1.5	10.78	2.20%	10.81	1.50%
T150-T150	3	0	4.50	0.00%	4.60	0.00%

	6	0	9.02	0.00%	9.19	0.00%
	9	0	13.54	0.00%	13.79	0.00%
	3	0.5	4.63	2.69%	4.71	2.46%
	6	0.5	9.14	1.33%	9.31	1.25%
	9	0.5	13.66	0.87%	13.91	0.84%
	3	1	4.75	5.45%	4.82	4.76%
	6	1	9.26	2.68%	9.42	2.47%
	9	1	13.78	1.76%	14.02	1.66%
	3	1.5	4.88	8.26%	4.92	6.94%
	6	1.5	9.38	4.04%	9.53	3.64%
	9	1.5	13.90	2.66%	14.13	2.47%
T190-T150	3	0	5.30	0.00%	5.24	0.00%
	6	0	10.63	0.00%	10.47	0.00%
	9	0	15.98	0.00%	15.71	0.00%
	3	0.5	5.46	2.94%	5.42	3.49%
	6	0.5	10.78	1.45%	10.66	1.79%
	9	0.5	16.13	0.95%	15.90	1.21%
	3	1	5.61	5.95%	5.59	6.70%
	6	1	10.93	2.91%	10.84	3.51%
	9	1	16.28	1.91%	16.09	2.38%
	3	1.5	5.78	9.00%	5.74	9.68%
	6	1.5	11.09	4.40%	11.01	5.16%
	9	1.5	16.44	2.87%	16.26	3.52%
T235-T150	3	0	6.45	0.00%	6.15	0.00%
	6	0	13.00	0.00%	12.29	0.00%
	9	0	19.64	0.00%	18.43	0.00%
	3	0.5	6.66	3.26%	6.58	7.00%
	6	0.5	13.20	1.58%	12.74	3.68%
	9	0.5	19.84	1.02%	18.89	2.50%
	3	1	6.88	6.58%	6.94	12.95%
	6	1	13.41	3.18%	13.15	7.04%
	9	1	20.05	2.06%	19.33	4.84%
	3	1.5	7.09	9.94%	7.26	18.18%
	6	1.5	13.62	4.80%	13.53	10.13%
	9	1.5	20.25	3.11%	19.73	7.05%

APPENDIX 3

Collision case T190-T150

Input data

Flexural strength $\sigma_f := 580 \cdot 10^3$ Pa

Elastic modulus $E_i := 5 \cdot 10^9$ Pa

Density of water $\rho_w := 1004$ $\frac{kg}{m^3}$

Density of ice $\rho_i := 900$ $\frac{kg}{m^3}$

Ice thickness $h_i := 1.5$ m

Ice-hull friction $\mu := 0.1$

Acceleration of gravity $g := 9.81$ $\frac{m}{s^2}$

Slope angle $\alpha := 1 deg$

Density difference $\delta\rho := (\rho_w - \rho_i)$

For deformation energy calculation:

Length(preferably midship length) $L_{mid} := 135$ m estimated

Draft $T := 9.2$ m

Mass of the striking ship $M_A := 46082000 \cdot 1.05$ kg

Mass of the struck ship $M_B := 27954000 \cdot 1.47$ kg

Speed of the striking ship $V_A := 3$ m/s

Stiffness $k := \frac{0.5 \cdot 1.4 \cdot 10^8}{6 \cdot 1.6} = 7.292 \times 10^6$ N/m

$k1 := \left(\frac{1.4 \cdot 10^8}{6 \cdot 1.6}\right) = 1.458 \times 10^7$ N/m

Breaking load component

$$\xi := \frac{\sin(\alpha) + \mu \cdot \cos(\alpha)}{\cos(\alpha) - \mu \cdot \sin(\alpha)} = 0.118$$

$$H_B := 0.68 \cdot \xi \cdot \sigma_f \cdot \left(\frac{\rho_w \cdot g \cdot h_i^5}{E_i}\right)^{0.25} = 2.886 \times 10 \frac{N}{m}$$

Ride-down force component

Height from waterline to the bottom of stucture(Draft)

$z := T = 9.2$ m

$$H_R := z \cdot h_i \cdot \delta\rho \cdot g \cdot (\sin(\alpha) + \mu \cdot \cos(\alpha)) \cdot \left(\frac{\sin(\alpha) + \mu \cdot \cos(\alpha)}{\cos(\alpha) - \mu \cdot \sin(\alpha)} + \frac{\cos(\alpha)}{\sin(\alpha)}\right) = 9.492 \times 10^4 \quad \frac{N}{m}$$

Horizontal ice force

$q_{Croasdale} := H_B + H_R = 9.781 \times 10^4$ $\frac{N}{m}$

Parameter C value for line load

$l_c := 15$ m

$s := 0.35$ m frame spacing

Deriving C value from line load equation:

$$C_1 := \frac{q_{Croasdale}}{\left(\frac{l_c}{s}\right)^{-0.71}} = 1.41 \times 10^6 \quad \frac{N}{m}$$

Ice load from line load

$$q_{ice}(L) := C_1 \cdot \left(\frac{L}{s}\right)^{-0.71} \cdot 2.6$$

$L := 0, 0.01 .. 150$

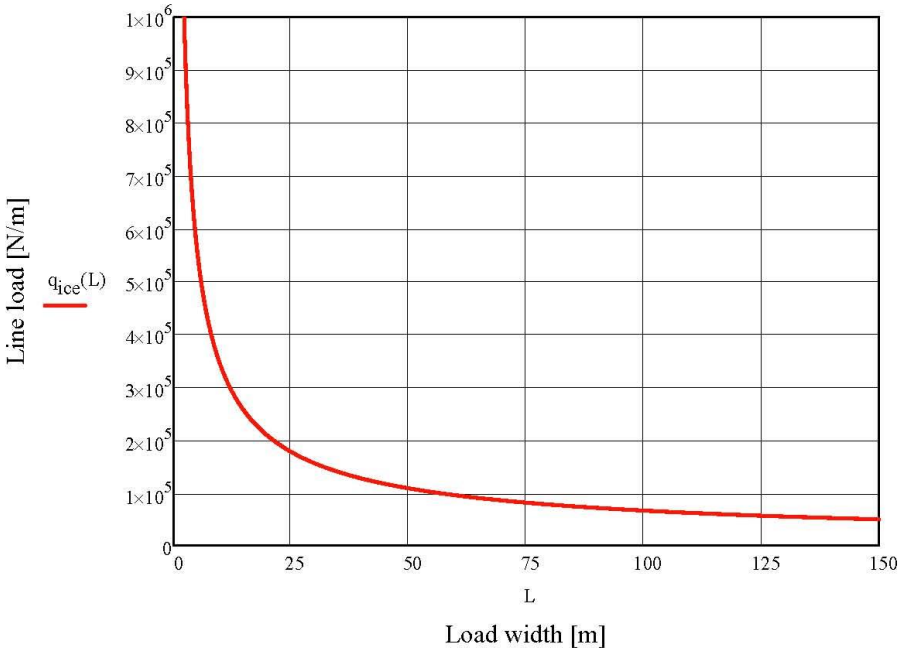

Getting ice load by multiplying line load with the length:

$$F_{ice} := q_{ice} \cdot L \cdot 2.6$$

Thus, the total ice load is:

$$F_{ice} := C_1 \cdot \left(\frac{L_{mid}}{s}\right)^{-0.71} \cdot L_{mid} \cdot 2.6 = 7.214 \times 10^6 \text{ N}$$

Ice mass derivation through energy balance equation:

$$M_{ice} := \frac{M_A \cdot V_A^2}{2} = \frac{1}{2} \cdot \frac{M_A \cdot (M_B + M_{ice})}{M_A + M_B + M_{ice}} \cdot V_A^2 + \frac{M_A \cdot \left(\frac{M_A \cdot V_A}{M_B + M_A + M_{ice}}\right)^2}{2} \ldots \quad \text{solve}, M_{ice} \rightarrow$$

$$+ \frac{M_B \cdot \left(\frac{M_A \cdot V_A}{M_B + M_A + M_{ice}}\right)^2}{2} + \left[F_{ice} \cdot \frac{M_A \cdot \sqrt{2 \left[\frac{1}{2} \cdot \frac{M_A \cdot (M_B + M_{ice})}{M_A + M_B + M_{ice}} \cdot V_A^2 \right]}}{k} \right]$$
$$2 \cdot (M_B + M_{ice})$$

Thus, ice mass is following:

$$M_{ice} = \begin{pmatrix} -1.61 \times 10^{7} \\ -3.983 \times 10^{7} \\ 1.862 \times 10^{7} \end{pmatrix} \quad \text{kg}$$

Knowing the ice mass it is possible to calculate deformation energy due to the collision, which is calculated as follows:

$$E_{Def} := \frac{1}{2} \frac{M_A \cdot (M_B + \max(M_{ice}))}{M_A + M_B + \max(M_{ice})} \cdot V_A^{\,2} = 1.203 \times 10^{8} \quad \text{J}$$

Common velocity and time

$$V_{com} := \frac{M_A \cdot V_A}{M_B + M_A + \max(M_{ice})} = 1.343 \quad \text{m/s}$$

$$t_{com} := \frac{\sqrt{\frac{E_{Def} \cdot 2}{k}}}{\left[V_A - \frac{M_A \cdot V_A}{(M_A + M_B + \max(M_{ice}))} \right]} = 3.466 \quad \text{s}$$

Penetration depth and ships displacement's

$$\delta := \sqrt{\frac{E_{Def} \cdot 2}{k}} = 5.744 \quad \text{m}$$

$$X_B := \frac{M_A \cdot \sqrt{\frac{2 \cdot E_{Def}}{k}}}{2 \cdot (M_B + \max(M_{ice}))} = 2.327 \quad \text{m}$$

$$X_A := \left(V_A - \frac{V_{com}}{2} \right) \cdot t_{com} = 8.071 \quad \text{m}$$

Contact force

$$F_C := \frac{E_{Def} \cdot 2}{\delta} = 4.188 \times 10^{7} \quad \text{N}$$

Checking balance equation :

$$E_0 := \frac{M_A \cdot V_A^{\,2}}{2} = 2.177 \times 10^8 \quad \text{J}$$

$$E_0 := E_{Def} + \frac{M_A \cdot \left(\frac{M_A \cdot V_A}{M_B + M_A + \max(M_{ice})} \right)^2}{2} \ldots = 2.177 \times 10^8$$

$$+ \frac{M_B \cdot \left(\frac{M_A \cdot V_A}{M_B + M_A + \max(M_{ice})} \right)^2}{2} + F_{ice} \cdot \frac{M_A \cdot \sqrt{\frac{2 \left[\frac{1}{2} \cdot \frac{M_A \cdot (M_B + \max(M_{ice}))}{M_A + M_B + \max(M_{ice})} \cdot V_A^{\,2} \right]}{k}}}{2 \cdot (M_B + \max(M_{ice}))}$$